Available online at www.sciencedirect.com
ScienceDirect
Trans. Nonferrous Met. Soc. China 33(2023) 969−996
Transactions of Nonferrous Metals Society of China
www.tnmsc.cn

# Research status and quality improvement of wire arc additive manufacturing of metals

Yan-peng LI[1,2], Chang-rui WANG[1,3], Xiao-dong DU[4], Wei TIAN[1], Tao ZHANG[5,6], Jun-shan HU[1], Bo LI[1], Peng-cheng LI[1], Wen-he LIAO[7]

1. College of Mechanical and Electrical Engineering, Nanjing University of Aeronautics and Astronautics, Nanjing 210016, China;
2. School of Aerospace, Transport and Manufacturing, Cranfield University, MK43 0AL, United Kingdom;
3. State Key Laboratory of Advanced Welding and Joining, Harbin Institute of Technology, Harbin 150001, China;
4. No. 29 Research Institute of CETC, Chengdu 610036, China;
5. Light Alloy Research Institute, Central South University, Changsha 410083, China;
6. State Key Laboratory of High Performance Complex Manufacturing, Central South University, Changsha 410083, China;
7. School of Mechanical Engineering Nanjing University of Science and Technology, Nanjing 210094, China

Received 25 January 2022; accepted 18 July 2022

**Abstract:** Wire arc additive manufacturing (WAAM) is a kind of additive manufacturing technology with excellent development potential in recent years. This work aims to summarize the current research status and challenges in WAAM and provide quality improvement methods. The research status of WAAM in surface finish and forming accuracy, microstructure and mechanical properties, residual stress and deformation, porosity and other defects is given. The methods of eliminating the above shortcomings and improving the microstructure and mechanical properties are summarized from pre-processing, on-line processing and post-processing perspectives. It is concluded that there are still many challenges to the widespread adoption of WAAM, and various perspectives may be needed to achieve this. The development of path planning and slicing algorithm, the combination of online monitoring systems with existing WAAM equipment, and composite post-processing technology will be the key research directions in the future.

**Key words:** wire arc additive manufacturing; material property improvement; process parameter control; in-process monitoring; post-treatment

## 1 Introduction

### 1.1 Background

With the development of the aerospace industry, the demand for large-scale, integrated, lightweight, and complex manufacturing is increasing, and higher requirements have been put forward for metal materials performance. The traditional manufacturing mode is difficult to meet the requirements of high efficiency and low cost.

Additive manufacturing (AM) is a new manufacturing technology with excellent development potential, which has attracted the interest of a large number of researchers. Unlike traditional manufacturing, AM does not make parts by removing materials, reducing the waste of raw materials, and making AM attractive at cost. In AM, raw materials are heated to a molten state and deposited ‘layer by layer’ along the predetermined

**Corresponding author:** Chang-rui WANG, Tel: +86-15952086703, E-mail: crwang@nuaa.edu.cn;
Wei TIAN, Tel: +86-13851662331, E-mail: tw_nj@nuaa.edu.cn
DOI: 10.1016/S1003-6326(23)66160-6

path, forming the desired shape [1−3]. AM is highly flexible because it does not require custom molds or special tools, and the manufacturing process can be adjusted at any time [4,5]. This realizes digitization, intellectualization, and parallelization [2]. As a non-contact manufacturing process, AM is not limited by the shape/construction of the parts, so it is especially suitable for manufacturing complex parts [3]. These characteristics make AM competitive in the fast, efficient, near-net forming of large and complex components. In the future, AM will likely replace traditional manufacturing method and become the mainstream manufacturing technology.

### 1.2 Genres of AM

AM technology can be divided into different types according to the heat sources and material supply modes. Main AM technology includes selective laser melting (SLM), electron beam melting (EBM), laser engineered net shaping (LENS), electron beam freeform fabrication (EBFF), and wire and arc additive manufacturing (WAAM). The characteristics of these AM technologies are given in Table 1.

SLM and EBM are powder bed fusion (PBF) technologies, and these techniques produce parts by melting metal powder laid on a powder bed. LENS, EBFF and WAAM are direct energy deposition (DED) technologies. Unlike PBF, in DED, raw materials are sent into the heat source affected zone to produce components. The advantage of PBF is the high precision, and this is because DED doesn't have powder support [4]. However, the DED has a high deposition rate, so it has great application value in making significant components [5].

SLM is the most widely used laser-based AM technology, suitable for various metal materials and metal matrix composite materials [6], commonly used in industrial manufacturing, biomaterial, medical fields, and so on [7]. SLM processes have high-speed heating and cooling rates [8], the components have refined grains, and mechanical properties can reach the forging level [9,10]. In addition, it also has the advantages of high material utilization and forming accuracy [11,12], attractive in precision manufacturing, when raw material costs are high. Electron beam is another common heat source with a high energy density [13]. EBMS can produce components quickly with low participation stress levels [14,15], and LENS has the advantage in the microstructure of manufacturing components because of the precise control of process parameters [16]. EBFF is another DED technology, which is the preferred AM technology for manufacturing refractory and active metal materials [17,18]. Compared with these AM technologies, WAAM has a higher deposition rate and is more environmentally friendly [19,20]. In addition, WAAM can use existing arc welding equipment, so the hardware cost is lower than that of other AM systems [21].

## 2 State-of-the-art

Although the performance of WAAM-manufactured components is comparable to that of conventionally-manufactured components in many cases, some deficiencies still need to be addressed. The surface finish of WAAM-manufactured components needs to be improved; high level of tensile residual stress and deformation, voids, cracking and other defects should also be avoided. There are many reasons for these defects, such as poor path planning, unstable welding pool dynamics caused by poor parameter setting, thermal deformation caused by heat accumulation, environmental impact, and equipment failure. The details of these common defects are discussed in this section.

**Table 1** Characteristics of different metal additive manufacturing

| AM technology | Heat source | Process type | Material form | Manufacturing environment | Component size |
|---|---|---|---|---|---|
| SLM | Laser | PBF | Powder bed | Inert gas | Small/Medium |
| EBM | Electron beam | PBF | Powder bed | Vacuum | Small/Medium |
| LENS | Laser | DED | Powder feeding | Inert gas | Medium/Large |
| EBFF | Electron beam | DED | Wire feeding | Vacuum | Large |
| WAAM | Arc | DED | Wire feeding | Inert gas | Ultra-large |

PBF−Powder bed fusion; DED−Direct energy deposition

### 2.1 Surface finish and dimensional accuracy

Macroscopically, the factors in evaluating WAAM quality mainly include surface finish and forming accuracy. The indexes in assessing surface quality include oxidation degree and surface roughness.

Oxidation is a defect worthy of attention in WAAM. Active metal materials commonly-used in aerospace structures, such as Ti−6Al−4V and aluminum alloys, easily react with oxygen at high temperatures to form oxides. As mentioned above, WAAM is a process of accumulation, and these oxides will enter the deposition layers during the remelting process, affecting the mechanical properties of the WAAM components [22]. YUE et al [23] pointed out that titanium oxidizes to form Ti02 when the temperature exceeds 500 °C. When this material with high hardness and high brittleness diffuses into the matrix, it will seriously affect the ductility and fatigue properties of titanium. In WAAM, aluminum reacts with oxygen to form an $Al_2O_3$ layer on the weld bead surface. However, if the process parameters are abnormal, the material may have uneven white accumulation. This abnormal oxidation phenomenon will change the mechanical properties of material, thus affecting the quality of the final part [24]. For Al−Mg alloy, MgO generated by oxidation weakens the solution strengthening effect, thus reducing the mechanical properties of the material. In addition, $H_2$ is produced during the oxidation process, which may increase the pores in the material [25].

As the molten pool is in a weak constrained state, and its ability to suppress complex disturbance is low, the stability of WAAM is insufficient. As a result, WAAM has some deficiencies in surface finish and dimensional accuracy [26,27]. This affects the mechanical properties (such as fatigue behavior, corrosion resistance, and creep life) and functional properties (such as friction, wear, reflection, heat conduction, and lubrication) of WAAM-manufactured parts. More seriously, this can lead to instability in subsequent deposition processes, resulting in defects such as pores, voids, and delamination, and reducing strength and fatigue life [28]. Some scholars have pointed out that the macroscopic accuracy of WAAM is strongly dependent on process parameters. Proper control of heat input and heat accumulation of deposition layers is beneficial to improving the surface finish of WAAM components [29].

In WAAM, welding voltage is unstable in the arc starting and extinguishing areas. In addition, the molten liquid metal is subjected to a combination of gravity, surface tension, and support force [30]. These factors lead to the height difference between arc starting and arc extinguishing points, as shown in Fig. 1. With the accumulation of errors, the material cannot obtain a protective atmosphere, resulting in oxidation and porosity, as shown in Fig. 1(b). What's worse, the arc torch may collide with the deposit when it returns, resulting in actuator end precision loss or even damage to welding equipment, as shown in Fig. 1(c).

### 2.2 Microstructure

Different types of microstructures can be observed in WAAM parts, and this is due to the difference in component undercooling. In WAAM, the solidification rate (SR) and local temperature gradient (TG) are the main factors affecting the component supercooling. Specifically, a higher TG/SR ratio results in the transformation of grains into columnar crystals. On the contrary, the grains are transformed into equiaxed grains. For a single deposition layer, the top is in direct contact with air, with high heat exchange efficiency and a high cooling rate, and grains solidify before they fully grow and are small in size. In the bottom, the material can dissipate heat through the former layers and substrate, so the grain size in this area is also refined. However, in the middle area, thick columnar crystals are formed due to the lack of cooling [31].

After the deposition, a kind of alternating structure is formed inside the WAAM component, as shown in Fig. 2(f). ZHOU et al [32] studied this structure in detail and found that it was a typical non-uniform band structure with alternating equiaxed and columnar crystals. The formation of this structure is as follows. During the deposition of the ($N$+1)th layer, the top of the $N$th layer was remelted, forming an inter-layer area. Since this area is in contact with the $N$th layer, which is cooled during interlayer cooling, SR is larger and equiaxed crystals are formed. However, in the inner-layer area, columnar crystals are formed along the vertical direction due to the slow cooling rate and the effect of gravity. As the deposition process goes

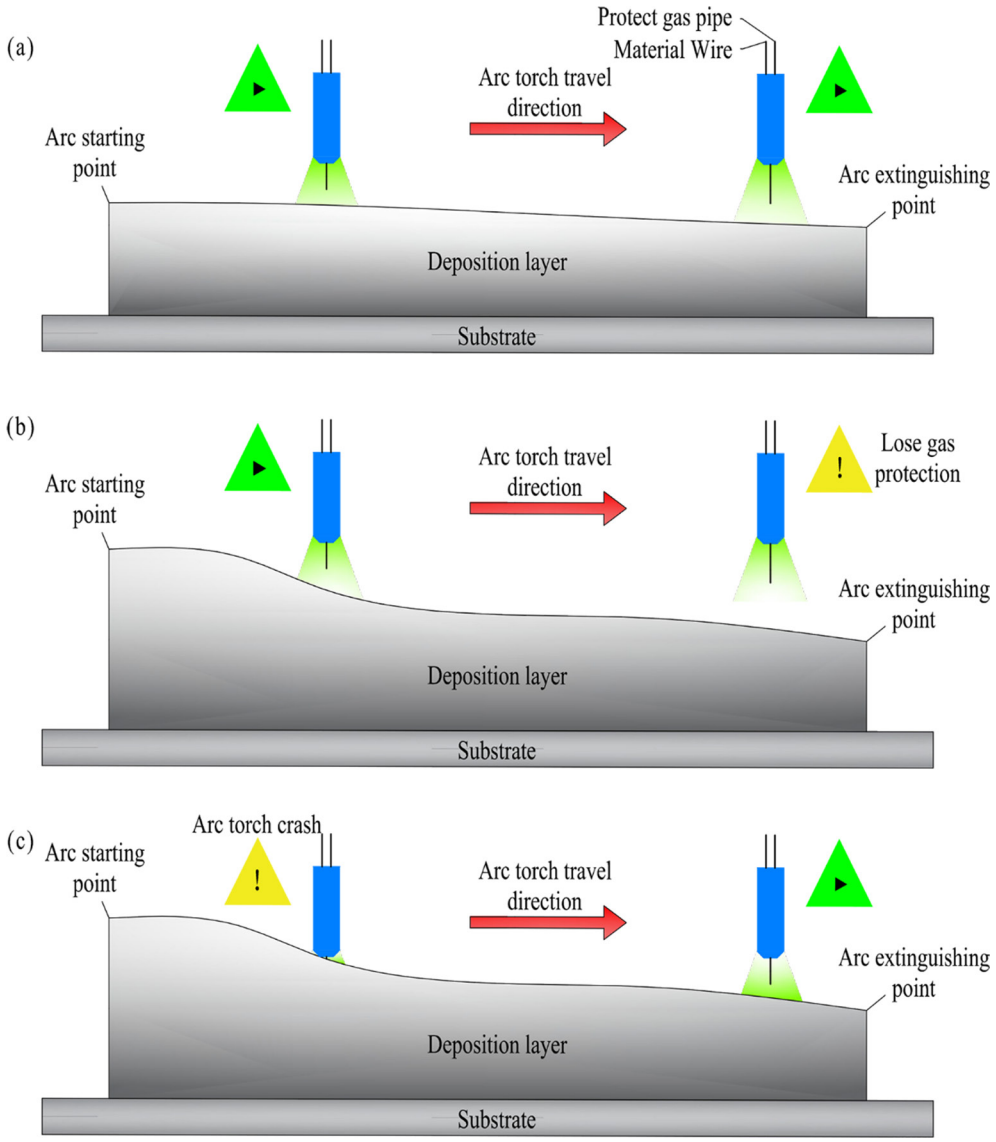


**Fig. 1** Side view of WAAM deposition layers with small (a) and large (b, c) height differences between arc starting and extinguishing points

on, the above steps are repeated, and finally, the columnar crystals and equiaxed crystals are alternately distributed in the component.

Similar to the deposition process, after the overlapping, a structure with an alternate distribution of inner-layer and inter-layer area is formed [33]. In the former, the grains grow along the heat conduction direction, and columnar crystals perpendicular to the fusion line are formed. In the latter, the grains cool rapidly, and equiaxed crystals are formed.

### 2.3 Mechanical properties

WAAM components have two disadvantages in mechanical properties. Firstly, there are a lot of coarse columnar crystals in WAAM components, which produce poor mechanical properties. The researchers point out that WAAM components are typical cast-state structures, and UTS and YS are not up to the standard of conventional forging parts [34]. At the same time, the difference in microstructure brings about differences in mechanical properties.

The highly unidirectional grain structure formed in the WAAM leads to the anisotropy of the mechanical properties [35−38], and may affect the corrosion and fatigue properties of the components [39]. LAGHI et al [40] found that elastic and shear modulus of WAAM components is significantly different in different directions.

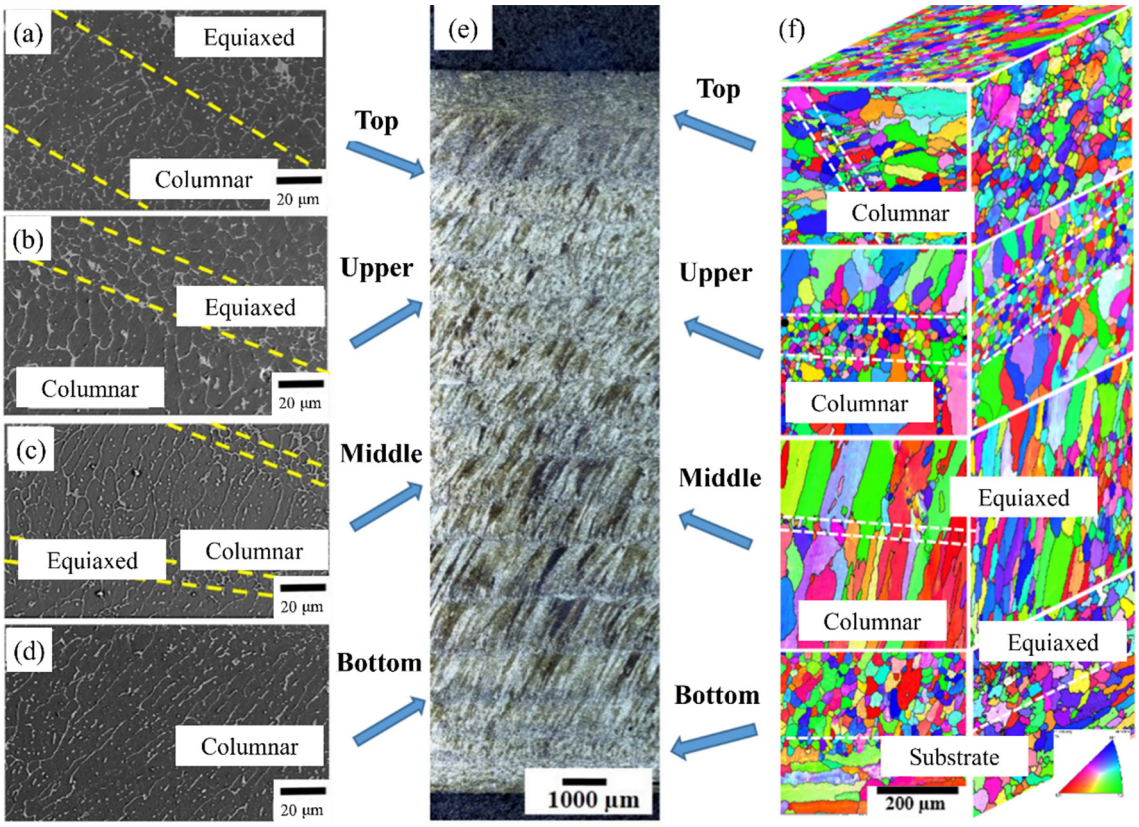


**Fig. 2** Microstructures of WC deposit: (a) Top zone; (b) Upper zone; (c) Middle zone; (d) Bottom zone; (e) Cross section; (f) 3D IPF photo [32]

SEOW et al [41] found that the tensile property of WAAM-718 alloy is diverse in different directions. HASSEL and CARSTEHSEN [42] tested the mechanical properties of WAAM components in different directions, and the results are shown in Fig. 3. In the direction of 90° and 0° to building direction (BD), the material shows lower strength and higher plastic deformation capacity. The part also shows different hardness values in different directions, as shown in Fig. 3(b). In the direction of 45° to BD, the hardness of the material is minor. GU et al [43] studied the mechanical properties of Al−Cu−Mg alloy WAAM components. As shown in Fig. 3(c), UTS and elongation have significant differences between horizontal and vertical directions, but the YS differs little in different directions. The tensile test indicates no significant difference in the tensile curves (Fig. 3(d)) in different directions before fracture, but a fracture in the vertical direction occurs earlier.

### 2.4 Residual stresses and deformation

In WAAM, internal stress occurs in the components due to arc heat and fixture. When these factors disappear, the stress caused by them still partially retains in the interior, that is, residual stress. The non-uniform distribution of the temperature field in WAAM is the main reason for residual stress formation [44].

The residual stress sometimes does not immediately show defects but gradually superposes with the working stress generated during the use, resulting in adverse effects such as deformation, delamination, cracking, and fatigue performance degradation. The plastic deformation will occur when the residual stress inside the component is huge, making the strain exceed the elastic limit. Residual stress also results in warping, delamination, and loss of edge tolerance [45,46]. Sometimes the residual stress of WAAM components is even close to its yield strength (YS), affecting fatigue performance and service life [47]. When the residual stress exceeds the tensile strength (TS), the parts will crack and cause economic losses. When the residual stress is between YT and TS, plastic deformation will occur in the material [48], which affects the dimensional accuracy and assembly performance.

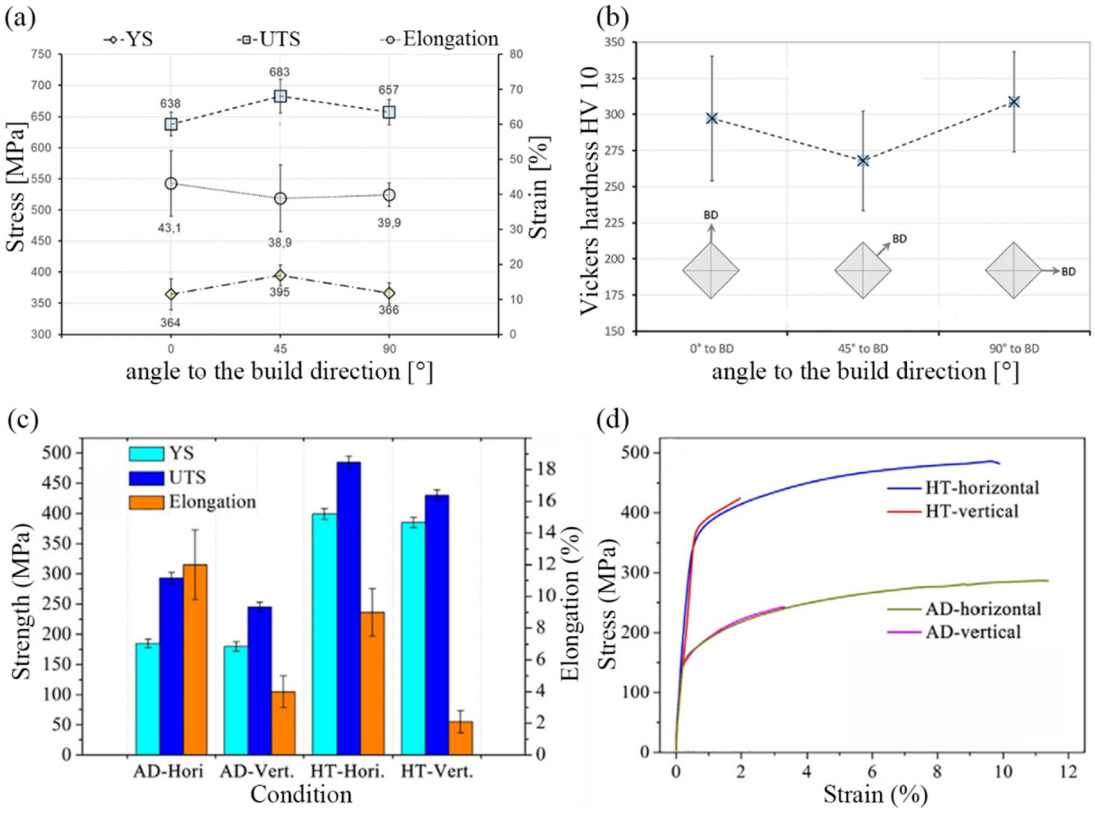


**Fig. 3** Mechanical properties (a) and Vickers hardness (b) of WAAM specimen in different directions; Tensile properties [42] (c) and stress−strain curves [43] (d) of as-deposited (AD) and heat-treated (HT) WAAM parts

### 2.5 Porosity and crack

Porosity is the most common but challenging defect in WAAM [49]. According to formation mechanism, porosity can be divided into raw material-induced porosity and process-induced porosity [50]. Raw material-induced porosity appears, because raw materials are contaminated with moisture, oils, and other hydrocarbons. During the deposition process, these pollutants are easily absorbed into the molten pool, and porosity is formed after solidification [51]. Process-induced porosity is caused by poor path planning or process parameters. Failure in path planning and process parameter selection makes the deposition process unstable, resulting in spatter or virtual welding, and finally causing porosity [52]. Another reason is that the high temperatures and pressures are generated by the arc split water vapor into hydrogen and oxygen ions, which are absorbed by the molten pool during deposition. The solidification process changes the solubility of hydrogen ions, and when it exceeds the solubility limit, hydrogen pores will be formed in the material [53]. Therefore, ensuring the cleanliness of WAAM raw materials and selecting appropriate process parameters are effective methods to avoid porosity. When subjected to tensile stress, micro-pores will gradually merge and eventually produce microcrack damage, thus reducing mechanical strength of components [54]. Stress concentration will occur around the porosity, which seriously affects the yield strength and fatigue strength of the material, and causes premature fracture. Porosity is also considered to cause mechanical anisotropy of WAAM forming parts [55].

Cracks are another common defects that may occur during WAAM. It is usually related to the thermal stress induced by AM process, and sometimes also related to the formation of micro-pores in the late curing stage [56]. Generally, cracks produced in WAAM are solidification cracks or grain boundary cracks [48]. The former is due to the different shrinkage rates of solidification in each part of the molten pool. The latter is due to the fact that the difference between the metal matrix and the precipitated phase, under the inner stress, produces cracking along grain boundaries. Crack is a defect that cannot be repaired by post-processing, which

will affect the strength and fatigue performance of the component [57]. Further expansion of crack may lead to fracture, resulting in unpredictable and irreversible losses.

## 3 Pre-processing before WAAM

Pre-processing means anticipating and planning the process or result of WAAM to avoid failures and improve final quality before it starts. The pre-processing methods generally include numerical simulation and path planning, which can improve forming accuracy and alleviate residual stress.

### 3.1 Numerical simulation

Understanding the evolution of physical fields in WAAM is very important for predicting microstructure evolution and mechanical properties of the final components. Many factors must be considered and designed in the WAAM process, including heat source parameters, arc torch travel speed, interlayer cooling time, etc. To optimize WAAM process, numerical simulation is essential. Unlike traditional experimental trial-and-error method, numerical simulation technology can save time and money [58]. As shown in Fig. 4, the numerical simulation of WAAM mainly is focused on temperature distribution, residual stress distribution and component deformation [59−61].

In recent years, studying temperature/residual stress distribution in WAAM process using numerical simulation has become a popular research direction. DING et al [62] replaced the traditional Gaussian heat source with a uniformly distributed heat source, which reduces the calculation

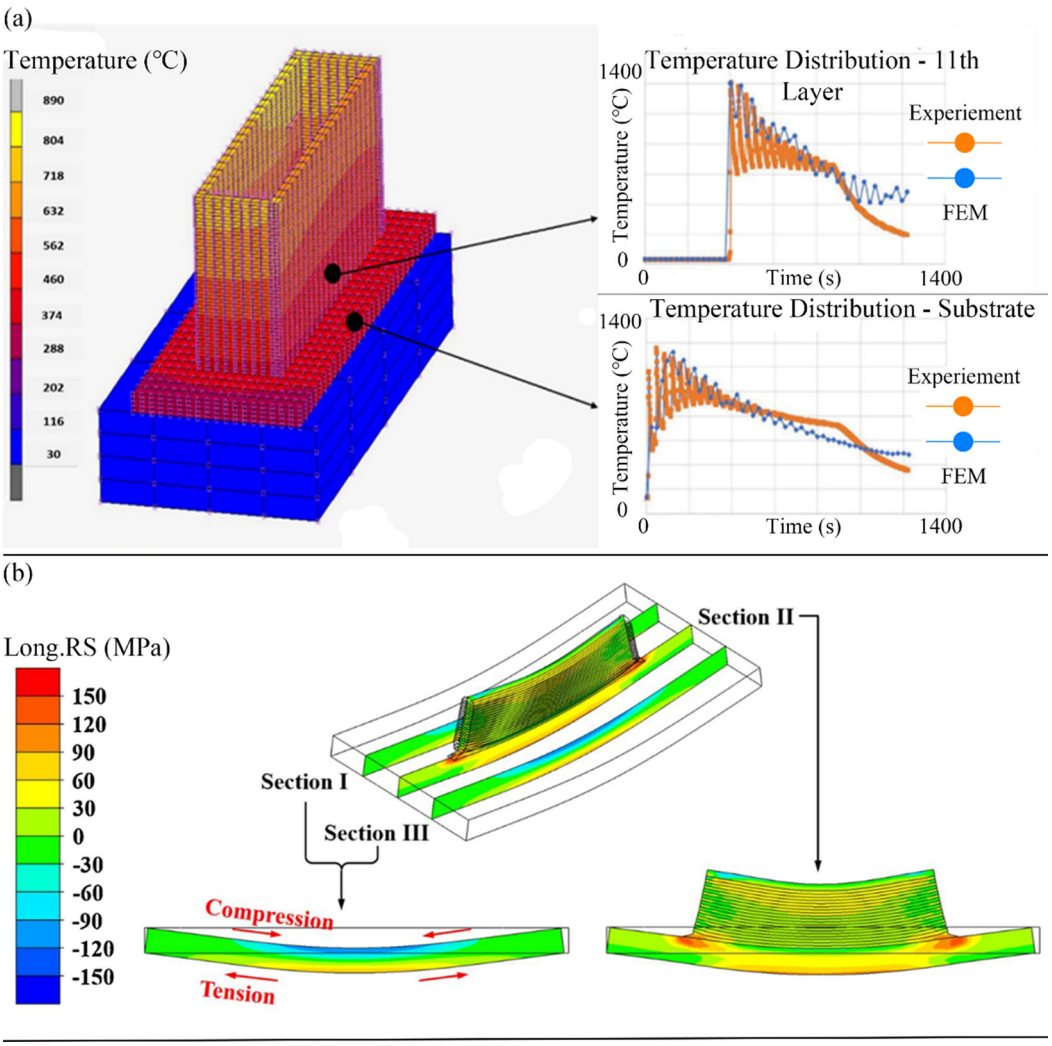


**Fig. 4** Cloud diagram of temperature field distribution and temperature−time curves at certain point of parts and substrate during WAAM [59] (a); Residual stress distribution and deformation in parts and substrate after WAAM process [60] (b)

amount of the finite element model. ABE et al [63] established a numerical simulation model of WAAM process to study the relationship between temperature and shape of the deposition layer. They deduced the optimal heat input conditions based on the finite element analysis (FEA) model. In terms of residual stress distribution, HUANG et al [64] found that longitudinal stress is produced near the root of the thin-wall build. The size of the high tensile stress area increases with the height of the component. HUANG et al [65] studied the influence of deposition path on the residual stress distribution, and the results showed that the stress field under reciprocating path deposition is more uniform than that under unidirectional path deposition. GORNYAKOV et al [66] proposed a short implicit transient rolling model. In this model, the implicit method is used for numerical solution, and the short-length model is used to achieve accurate stress−strain prediction, while the calculation time is reduced by 96.5%.

Some scholars want to determine appropriate WAAM process parameters through numerical simulation because of its economy and convenience. CADIOU et al [67] used COMSOL to simulate WAAM process. The advantage of this model is that it simulates the process of melting drop, and considers the electromagnetic and fluid flow and Joule effect. Therefore, this method can simulate the WAAM process more accurately. HEJRIPOUR et al [68] established a numerical model to analyze the effects of torch travel speed (TS) and wire feeding speed (WFS) on the homogenization of WAAM parts. The result showed that the composition of the fusion zone is more uniform with the increase of WFS. SAADATMAND and TALEMI [69] found that increasing TS can reduce the effects of heat input. LI and XIONG [70] found that with the rise of interlayer idle time, the stress cycle curve tends to be uniform, and the residual stress on WAAM component and substrate decreases significantly. HACKENHAAR et al [71] simulated the impact of air jet impingement on the temperature field of the whole part. The results showed that air jet impingement can effectively limit the temperature rise. This is because air jet impingement increases the convective heat transfer rate. OYAMA et al [72] thought interval durations in the WAAM process should be as short as possible to limit the structural distortion in the aluminium alloys.

### 3.2 Slicing algorithm

Researchers have done a lot of work on slicing algorithms. The main slicing algorithms can be divided into simple plane, surface, and multi-direction slicing algorithms. The simplest slicing algorithm is planar slicing algorithm, which is applied to simple models. The surface slicing algorithm makes the deposition path a continuous spatial curve, which can avoid the problem of poor precision caused by path discontinuity. ZHANG et al [73] used curved laminated section algorithm to manufacture complex nine-way tube structure. The multi-direction slicing algorithm is suitable for complex parts, is the most appropriate algorithm for WAAM [74], and allows the WAAM to proceed in different directions, eliminating the need for support [75].

The algorithm of WAAM control software has two types. One is directly generating fixed spatial coordinate information. This method cannot be adjusted and can cause a significant error in the manufacturing process. The other way is to use closed-loop control, which has higher flexibility and adaptability [76], and can eliminate the error in the WAAM process in real-time. ZHAO et al [77] developed a slicing algorithm to achieve self-adaptive control through the process parameters and the size of the part itself. REBAIOLI et al [78] developed a closed-loop control strategy. The sensors collect dimensional data and transmit it to the computer. When the error reaches a certain level, the slicing program re-slices, re-constructs contour, plans a new path and transfers the new path data to the robot.

ZHANG et al [73] proposed a slicing algorithm, and the working process is shown in Fig. 5. Firstly, the algorithm obtains the contour polygon by the intersection of triangular block and slicing plane. Next, the algorithm judges the order of these intersection points with normal vector and puts them into the ‘starting’ or “ending” arrays (Fig. 5(c)). Traversing these two arrays can improve treatment efficiency. Then, the contour of the sedimentary layer is obtained by interpolation algorithm, and finally, the deposition process is carried out along the designed path.

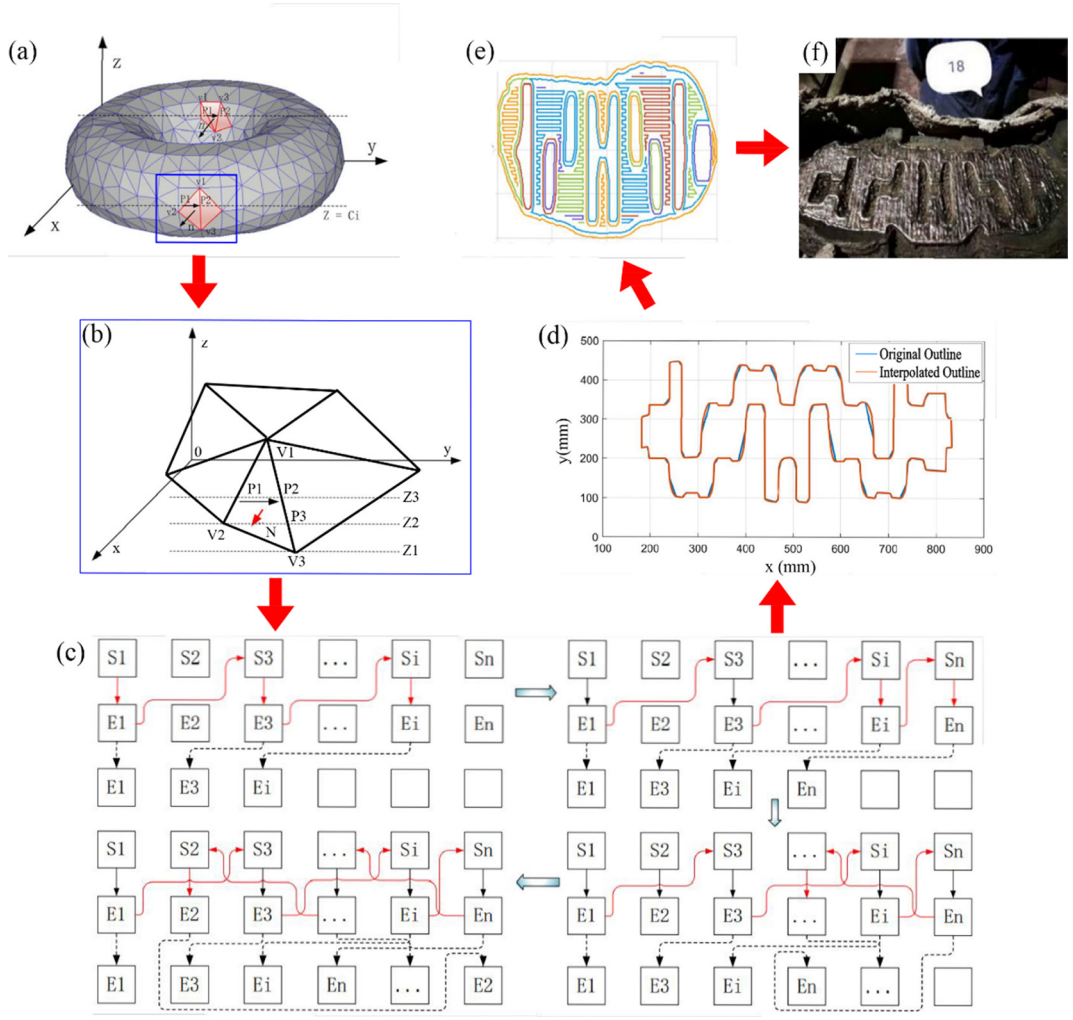


**Fig. 5** Slicing diagram of STL model: (a) Linear equation solving; (b) Intersection points solving; (c) Recombination of directed line segments of slices; (d) Contour of surface by using interpolation program; (e) Welding path of eighteenth layer; (f) Final result [73]

### 3.3 Path planning

Different deposit paths will affect the molding speed, precision, surface quality, microstructure, and performance of WAAM [79]. Typical deposit strategy includes raster, zigzag, contour, spiral, space-filling, grid, honeycomb, hexagonal, and Voronoi diagram-based infills (Fig. 6) [80].

DING et al [81] found that path planning based on the geometric features of components can effectively improve the forming quality and accuracy of components. DIOURTÉ et al [82] proposed a deposition strategy called continuous 3D path planning (CTPP), a 3D trajectory generation strategy for thin-walled and closed-loop complex structures. This planning method ensures that parts remain in good shape during WAAM. FENG et al [83] developed a new path planning method by combining fractal line filling method with bias filling method. The new method simplifies the complexity of the original algorithms and improves the forming efficiency. General Electric (GE) [84] combined WAAM and machine learning, using artificial intelligence technology to improve the manufacturing accuracy of WAAM parts.

It is essential to realize the support-free deposition of metal parts since the supporting structure is hard to remove. LIU et al [85] developed a support-free path planning method, as shown in Fig. 7(a). They divide components into internal solid (IS) and surface, and the surface is further divided into overhanging zone (OA) and non-overhanging zone (NOA). During deposition, NOA is deposited firstly as a support for OA, and

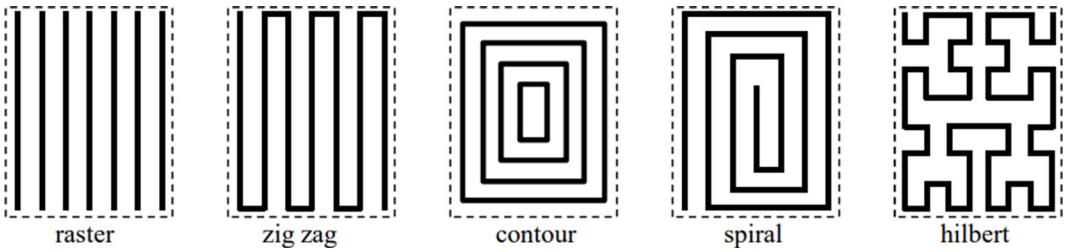


**Fig. 6** Common infill strategies in AM [80]

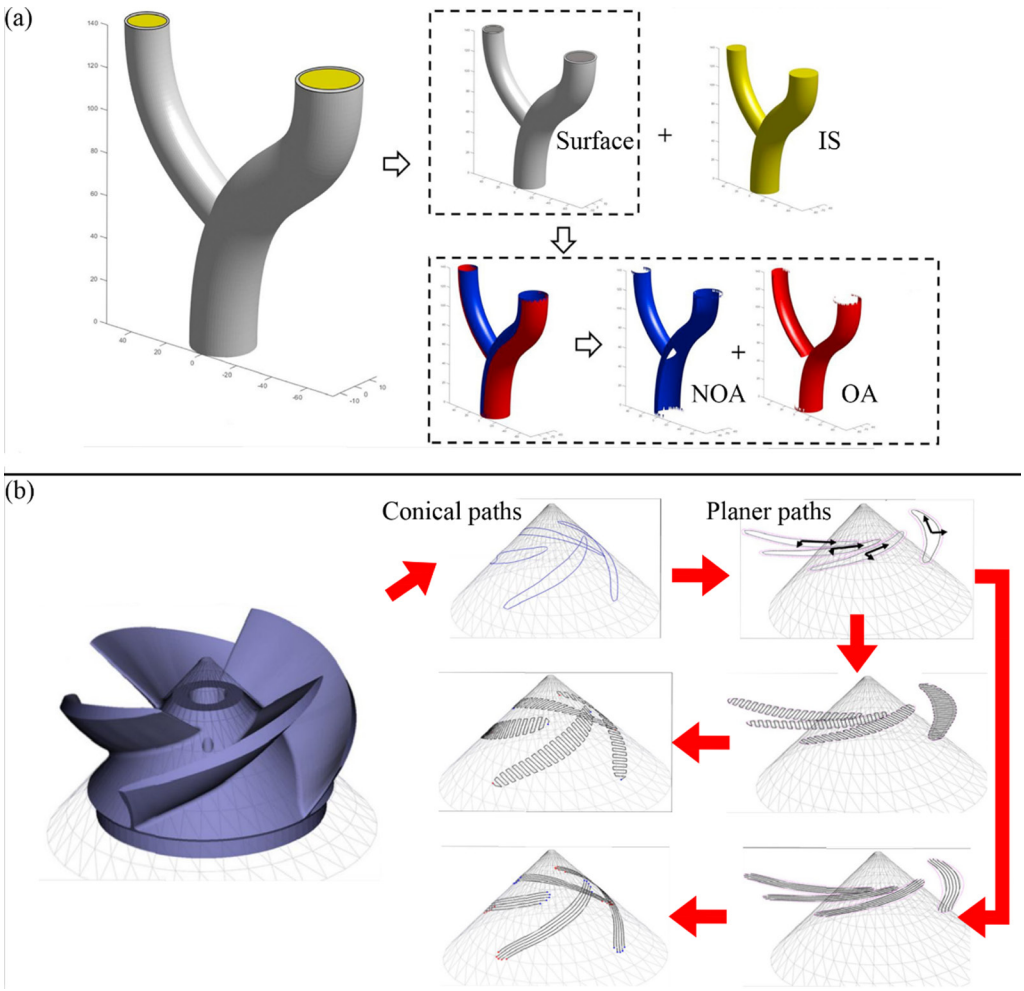


**Fig. 7** Schematic diagram of division of each part in process of support-free path planning [85] (a); Principal component analysis (PCA)-based path planning [86] (b)

further, OA is used as a support for IS. DAI et al [86] used principal component analysis (PCA) for path planning, as shown in Fig. 7(b). They found that the second principal component of a planar contour is a reasonable scanning direction to generate zigzag filling paths and parallel skeleton filling paths.

## 4 Online-processing during WAAM

Online-processing is the method that can maintain the process stability, reduce the failures and improve the quality of finished products through a series of operations such as monitoring, feedback and adjustment. Online-processing generally includes in-process monitoring, molten pool thermal management, process parameter control and other aspects, which positively affects the smooth and stable progress of WAAM, as well as the macroscopic morphology, microstructure and mechanical properties of the final product.

### 4.1 Thermal management

In the WAAM process, excessive heat input produces serious heat accumulation. The loss of thermal management leads to the instability of the molten pool, reduces the deposition rate, and produces uneven structure [87,88]. In WAAM, a large heat input leads to a slow cooling rate, providing sufficient time for grain growth. As a result, the strengthening effect of fine grain is weakened and the component strength is reduced [89,90].

Many scholars have studied the effect of heat input on WAAM components. DINOVITZER et al [91] studied the effects of current and TS on the morphology of weld bead, and with the increase of current, bead height decreases and bead width increases. This is because large heat input makes the material easier to spread out. KLEIN and SCHNALL [92] found that reducing welding current can decrease grain size. However, the mechanical properties of WAAM parts cannot be improved significantly by thermal management.

In addition to reducing the thermal power of the welding power supply, another idea is to increase the heat loss in WAAM, such as increasing the cooling time or using additional cooling processes/steps. Heat in WAAM is mainly dissipated through the heat transfer with the substrate, and the convection and radiation to the ambient environment [93]. But with the increase of layers, the heat dissipation through the substrate becomes more and more difficult, and the heat dissipation efficiency of convection and radiation is not high. As a result, heat accumulation becomes more serious, making WAAM process unstable and seriously affecting the quality of finished products. Introducing additional cooling can solve this problem.

WU et al [94] used $CO_2$ gas to cool the welding layers, and found that interlayer cooling can improve the hardness and strength of Ti−6Al−4V alloy. KARUNAKARAN et al [95] used a coolant to enhance the heat transfer efficiency between the deposition layers and the substrate, effectively reducing the thermal damage in WAAM parts. LI et al [96] studied the effect of cooling system on the morphology of welding beads. They found that the heat accumulation increases the width to height ratio (RWHT). After adding cooling device, the RWHT decreases. And with the increase of cooling device power, the value of RWHT further decreases.

### 4.2 External wire feeding

To reduce the negative impact caused by excessive heat input, in addition to reducing arc power and adding cooling, another idea is to increase the volume of the material fed into the arc heat-affected zone per unit time. LIU and XIONG [97] used external wires in the WAAM process, and the thermal damage decreased and the deposition efficiency increased. For the micro-structure, with the increase of the external filler wire feed speed (EFWS), the equiaxed dendrite size decreases as the material experiences supercooling and dendrite segregation. HAN et al [98] studied the effect of additional auxiliary wire on bead shape. They found that the height of the welding bead increases with the increase of $v_{fa}$ (feeding speed of auxiliary wire), but the width seems not to be affected. This is because when the other parameters are identical, increasing WFS does not change the affected area of arc heat.

The change of WFS does not significantly change the mechanical properties of material [97]. Grain size is an important factor affecting the mechanical properties [99,100]. This method can only refine the grains at the top of the deposition layer, which is a benefit to mechanical properties. But the increase of WFS also enlarges the area of columnar crystals in the middle and bottom area. The increase of columnar crystals area will offset the improvement of grains in the top area. Finally, there is no significant improvement in mechanical properties.

### 4.3 Cold metal transfer technology

Cold metal transfer (CMT) technology is a welding technology based on the short-circuit transition principle. CMT welding has four main steps. At first, the arc melts the metal wire. Under gravity, the droplets drop into the molten pool. Next, the arc is extinguished when the droplet contacts the molten pool, resulting in a sudden current drop. Then, the wire feeding system draws back the welding wire, accelerating the dropping of the droplet. Finally, the arc is reignited, and the process starts again. This “cold-hot-cold” cycle process is repeated until the welding is finished [101,102].

CMT can significantly reduce heat input and

splash in the welding process [103], and improve forming accuracy, morphology, microstructure and mechanical properties of WAAM parts. Compared with other heat sources, CMT-manufactured components have a refined microstructure and less anisotropy of mechanical properties. JIANG et al [104] fabricated 4043 aluminum alloy parts by CMT, and they found that the parts have a uniform microstructure and no anisotropy on mechanical properties. ELREFAEY [105] pointed out that compared with MIG welding, the grains of the workpiece manufactured by CMT were smaller, and the TS and elongation were higher. POSCH et al [106] found that using CMT can reduce the surface roughness. CONG et al [107] studied the effect of CMT technology on porosity in Al−6.3%−Cu components, and the results showed that the CMT produced less porosity due to smaller spatter and heat input.

### 4.4 In-process monitoring and control

To ensure the accuracy and stability of WAAM, in-process monitoring and control are needed. Based on sensor type, WAAM in-process monitoring system can be divided into visual sensing based, acoustic sensing based, spectral sensing based, and thermal sensing based systems.

The sensitivity of the visual system is not high because of the lag of visual sensor. XIONG et al [108] introduced the monitoring data of the previous layer into the current layer to improve the response speed of the control system. The spectrum generated by the arc contains a lot of information that can be used to evaluate the quality of WAAM. ZHANG et al [109] developed an in-process monitoring system for GTAW welding defects based on spectral analysis. The system consists of a spectrometer and a set of detector lenses. The abnormal oxidation region can be accurately found by detecting changes in the wavelength of the spectrum. JIA et al [110] developed a plasma arc welding sensor and control system based on efflux plasma voltage sensor. Further, they determined the linear relationship between welding current, efflux plasma voltage and weld width, and finally ensured the stability of welding process. Acoustic signals can be used to characterize arc stability, deposition process dynamics and changes within the material. The advantages of acoustic sensors are non-contact, non-destructive and flexible, making acoustic sensing become a competitive way of in-process monitoring. PAL et al [111] found that acoustic emission signals can reflect defects in the arc welding process. SHEVCHIK et al [112] used acoustic emission (AE) and machine learning (ML) to monitor the distribution of defects in the SLM process, thus improving the quality of finished products.

Ultrasonic detection is another commonly-used defect detection method, and it has the advantage of high sensitivity and high accuracy. RIEDER et al [113] conducted online ultrasonic measurement during AM and found that it can detect residual stress and porosity of materials. MA et al [114] developed a laser opto-ultrasonic dual (LOUD) detection device, as shown in Fig. 8(a). The system is equipped with a laser emitter, which produces laser ablating the surface of material, producing plasma and ultrasonic pulse, and thus generating spectral and ultrasonic signals. Ultrasonic signals and spectral signals are collected by an ultrasonic probe and a spectrometer. This system can detect residual stress distribution, element distribution and defects, as shown in Figs. 8(b−d). SUÁREZ et al [115] used thermal imaging to obtain dimensional images. Any defect can be located using image processing technology, which realizes the traceability of parts and avoids the propagation of defects. CHEN et al [116] pushed the existing infrared monitoring method to real-time detection and proposed a non-destructive detection method of multi-feature data fusion in process based on the WAAM process temperature field.

## 5 Post-processing after WAAM

Post-processing refers to applying some additional processes to the finished WAAM components, changing the surface finish, eliminating residual stress and deformation, reducing internal defects and improving mechanical properties. Post-processing generally includes plastic deformation, surface strengthening, compound subtractive manufacturing and heat treatment [117].

### 5.1 Rolling

Rolling is a widely-used technology to eliminate defects and improve microstructure and properties. Rolling imposes a huge load on the material to break the grains, refining the micro-

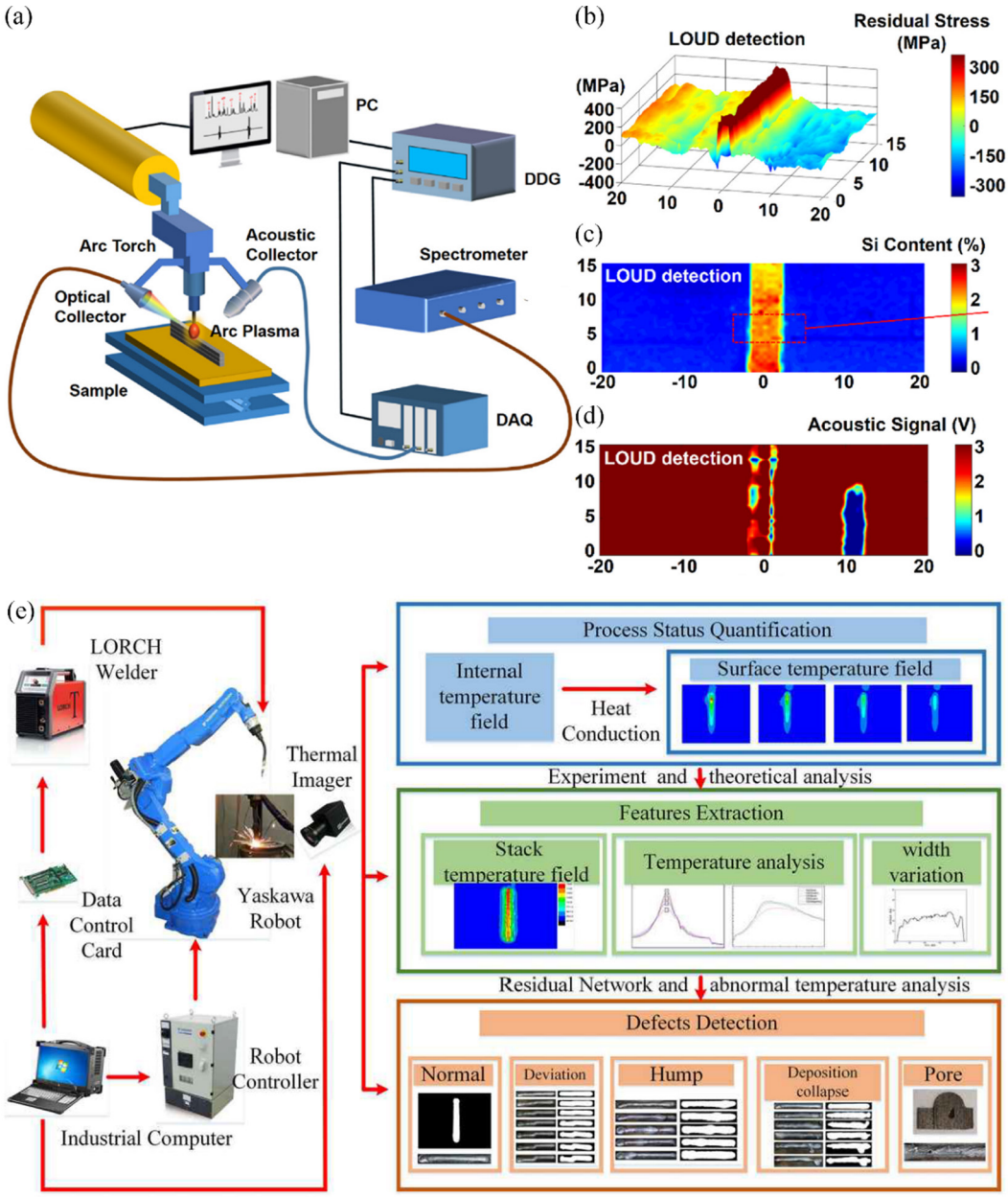


**Fig. 8** Schematic diagram of working principle of laser opto-ultrasonic dual (LOUD) device detection equipment (a); Using LOUD in-process monitoring equipment to detect residual stress distribution, element distribution, and defect in WAAM process [114] (b−d); Schematic diagram of WAAM in-process monitoring experimental device based on thermal imaging and process defect detection process [116] (e)

structure and improving the mechanical properties. In addition, rolling can reduce the harmful tensile stress formed in WAAM, thereby reducing part cracking and deformation [118,119], which has also been proven to weaken the texture in material, thereby decreasing the anisotropy [120].

5.1.1 In-process hot rolling

The plastic deformation of the material at high temperatures will produce a rise in dislocation density, resulting in work hardening, and thus improving the strength. In addition, hot rolling can also trigger a dynamic recrystallization (DRX) process, which significantly refines the micro-structure [121,122]. In addition, materials have low strength at high temperatures, so they can improve the rolling-effect-depth, and reduce the rolling force. In hot rolling, the roller is usually installed together with actuator, and the roller will roll the material immediately after it is deposited [123,124].

Rolling can alleviate the internal defects

and improve the mechanical properties of the material. SOKOLOV et al [125] found that many dislocations are formed after rolling, which is beneficial to recrystallization process. POPOVICH et al [126] found that hot rolling can increase UTS of copper alloy WAAM parts by 20%−25%. OH et al [127] studied the effect of hot rolling on the mechanical properties of 316L stainless steel, and found that hot rolling can increase the elongation of the material. XIE et al [123] found that hot rolling can significantly reduce defects formed within materials during WAAM. After the rolling treatment, the number and size of defects in the specimen are reduced, as shown in Fig. 9.

The rolling process parameters have an important influence on final result. QIU et al [128] found that increasing the rolling depth decreases grain size and the microstructure becomes more uniform. The tensile test shows that the fracture behavior of the component gradually changes from brittleness to toughness with the increase of rolling depth, indicating that rolling refines the microstructure.

5.1.2 Cold rolling

Cold rolling is relatively independent of the WAAM process, so it does not affect the stability of the WAAM process [129]. But due to the high strength of the material at low temperature, cool rolling needs a higher rolling force, which puts forward higher requirements for the rolling equipment. To improve the efficiency of cold rolling, TANGESTANI et al [130] used inter-layer cold rolling to improve the rolling depth. ABBASZADEH et al [61] found that increasing the rolling depth and the rolling force or decreasing the roller radius can increase plastic deformation.

Cold rolling can effectively break the coarse columnar crystals. MARINELLI et al [131] found an equiaxial structure formed after cold rolling. DONOGHUE et al [132] found that rolling can significantly refine the microstructure of WAAM walls. The degree of grain refinement increases with the increase of rolling force, as shown in Fig. 10(a). ZHANG et al [133] found that the columnar dendrites are broken and transform into equiaxial crystals by cold rolling. The average grain size decreases from 83 to 26.2 μm, as shown in Fig. 10(b). HÖNNIGE et al [134] found that inter-layer rolling can disrupt dendrite growth and make the microstructure more refined, as shown in Fig. 10(c).

Rolling can improve the residual stress distribution in WAAM-manufactured components. HÖNNIGE et al [135] studied the effect of rolling mode on component properties, as shown in Figs. 11(a, b). The results showed that vertical inter-pass rolling causes work hardening, thus improving the yield and tensile strength of the WAAM specimen. In comparison, side-rolling is very effective for controlling residual stresses and

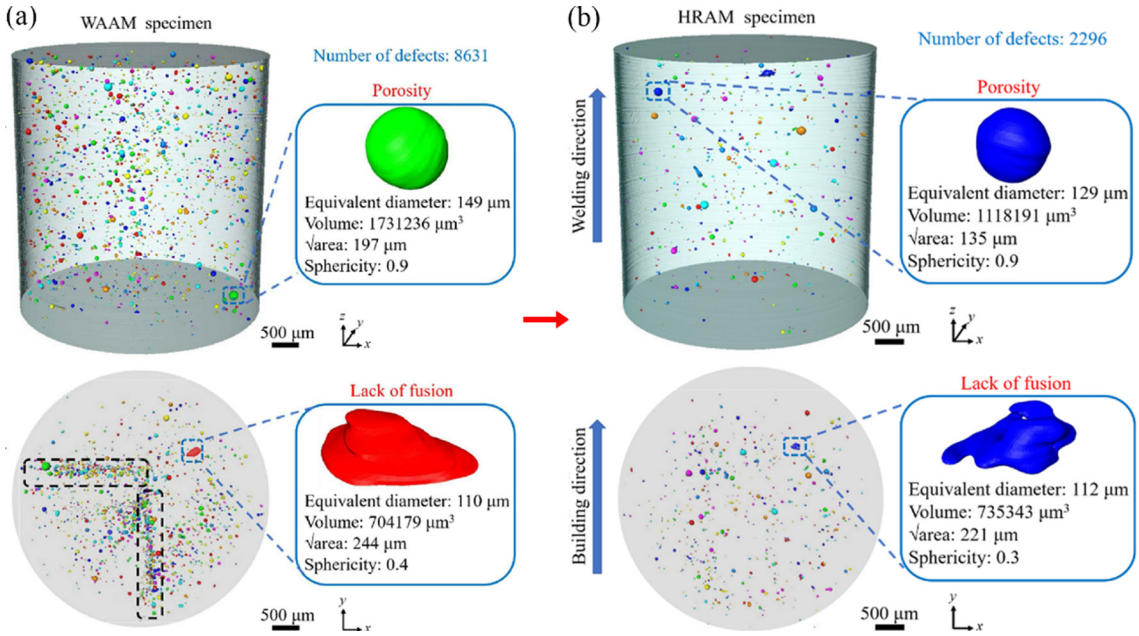


**Fig. 9** SR-μCT-based reconstructed volumes: (a) Without rolling; (b) After rolling [123]

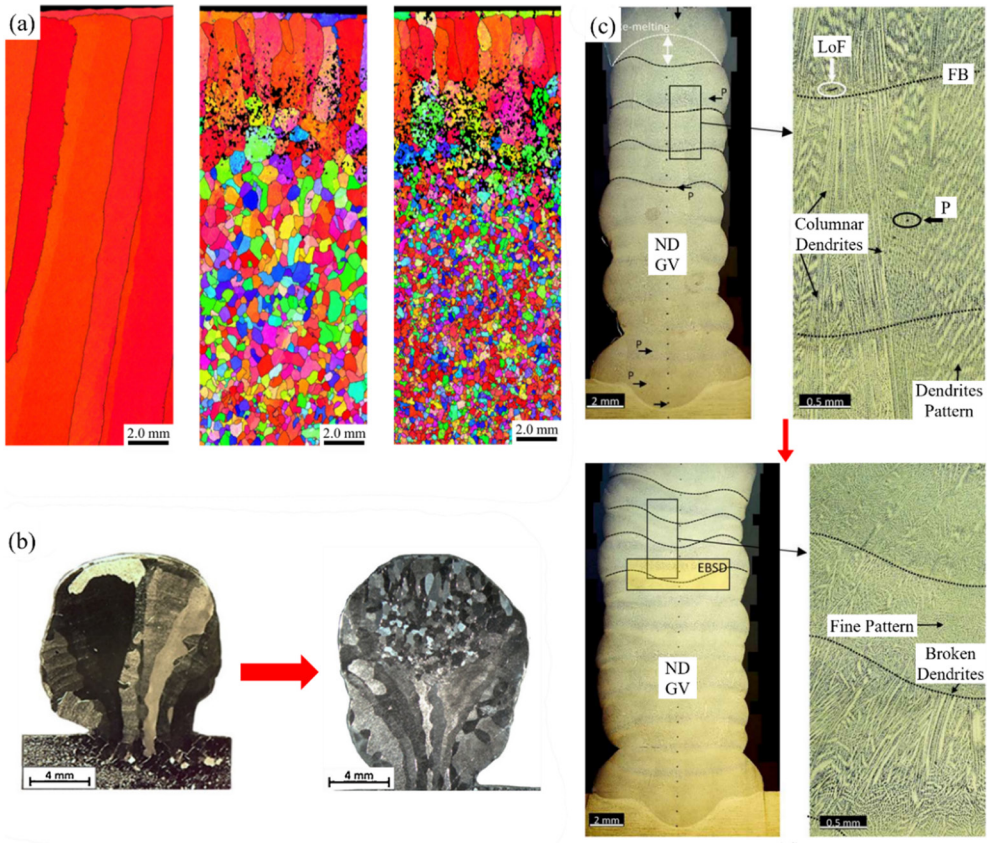


**Fig. 10** EBSD maps from undeformed control and rolled WAAM walls [132] (a); Optical micrographs of samples not rolled and rolled on top and between layers [131] (b); Microstructure characteristics of samples without rolling and with inter-pass rolling [134] (c)

distortion. TANGESTANI et al [130] found that rolling could transform the residual tensile stress inside WAAM parts into compressive stress. ABBASZADEH et al [61] established the rolling finite element model of 2319 aluminum alloy and found that increasing the rolling force and rolling radius can enlarge the residual compressive stress layer and increase the maximum residual compressive stress, as shown in Figs. 11(c, d). JU et al [136] studied the effect of interlayer rolling on the distribution of residual stress in WAAM Ti−6Al−4V alloy by finite element simulation. The results showed that the residual macroscopic stress in the metal and the overall stress in the sample are significantly reduced by interlayer rolling.

### 5.2 Surface strengthening

Surface strengthening generally includes laser shock peening (LSP), ultrasonic impact treatment (UIT), shot peening, etc. The principle of these methods is to use impact force to improve the quality of materials. Although the effect depth of surface strengthening technology is not considered, it has high flexibility, so it is suitable for parts with complex structures.

#### 5.2.1 LSP

LSP using a laser beam impacts the material, forms many dislocations and transforms the coarse columnar crystals into the fine equiaxed crystals. LSP can improve the fatigue resistance, wear resistance and corrosion resistance of the material. In addition, it can significantly reduce the harmful residual tensile stress and the porosity in the parts [137,138].

SUN et al [139] found that LSP can refine the microstructure significantly. CHI et al [140] using XRD and EBSD analyzed the effect of LSP on the microstructure of Ti17 WAAM parts, and the results are shown in Fig. 12. The decrease of grain size will increase the value of full width at half maximum (FWHM) [141]. In Fig. 12(b), after LSP, the increase of FWHM indicates a drop in grain size. In EBSD analysis, Kernel average misorientation (KAM) represents the degree of misorientation

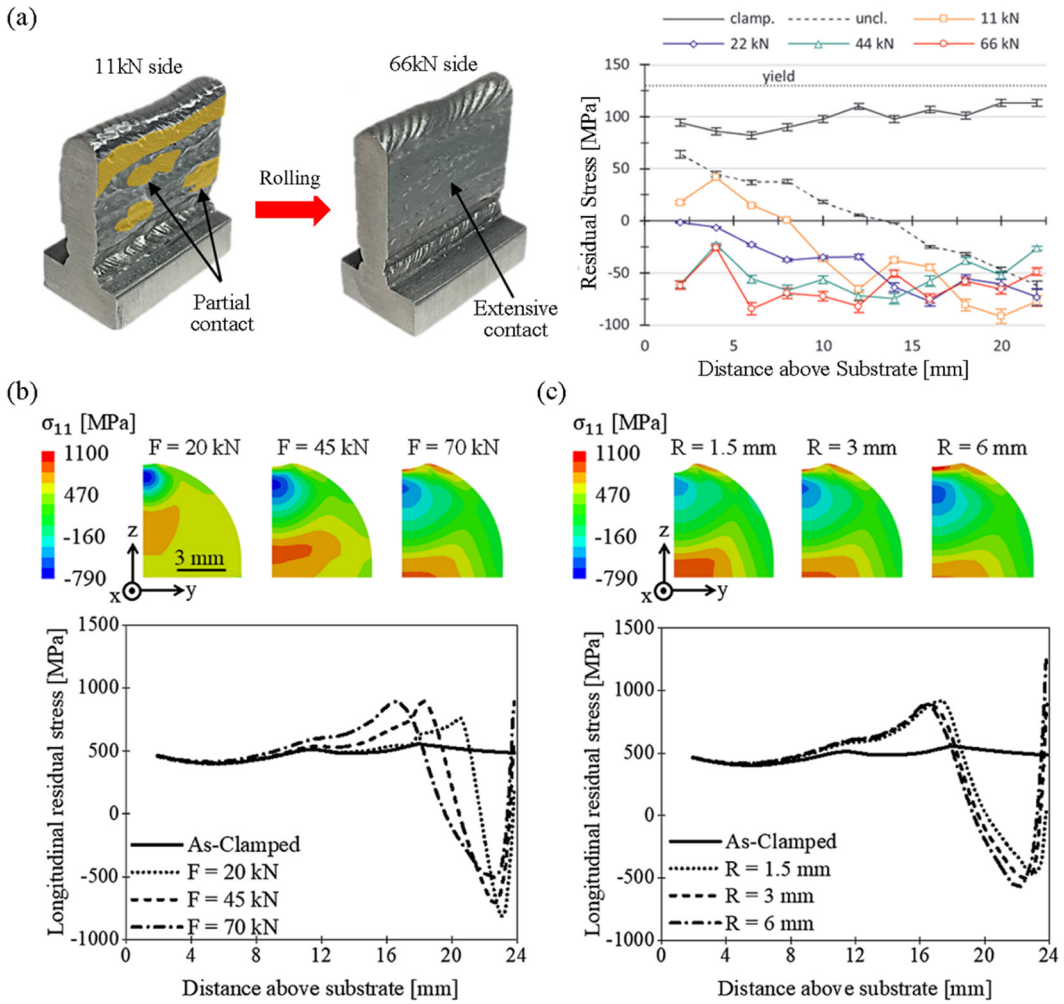


**Fig. 11** Wall shape and residual stress of side-rolled WAAM specimen [135] (a); Longitudinal residual stresses in Ti−6Al−4V after rolling for different rolling loads (b) and rolling radii (c) [61]

between adjacent points [142], and a high value of KAM indicates a significant degree of plastic deformation. As can be seen from Figs. 12(c−e), after LSP, the deformation in the specimen increases (the red area rises). From Figs. 12(f−h), after UIT, the KAM values grow to 2.40 after LSP, showing that LSP can produce plastic deformation of grain. SUN et al [143] studied the effect of LSP on the grain size and mechanical properties of WAAM 2319 aluminum alloy parts. After LSP, the average diameter of grains decreases by 50.2%, from 68.86 to 34.32 μm.

LSP can reduce the residual tensile stress formed during AM or transform it into compressive stress, thus preventing the deformation and cracking of parts and improving the hardness and fatigue resistance of the material. GUO et al [144] and LUO et al [145] had similar results: the residual compressive stress is generated after LSP, and the fatigue resistance is greatly improved. KALENTICS et al [146] found that LSP can change the tensile stress of specimens into compressive stress.

5.2.2 UIT

In UIT, ultrasonic vibrations are generated by an ultrasonic transducer and amplified by the concentrator. The concentrator pushes the pin to impact the sample surface at a high frequency [147]. After UIT, the treated area can be divided into three zones: (1) Core zone (CZ) with a depth of several microns. The grains in this region are sufficiently refined. (2) Plastic deformation zone (PDZ), with a depth of hundreds of microns. Plastic deformation occurs in this region, the residual tensile stress is transformed into compressive stress, and the micro-structure, mechanical, and fatigue properties are improved. (3) Stress relaxation zone (SRZ), with a

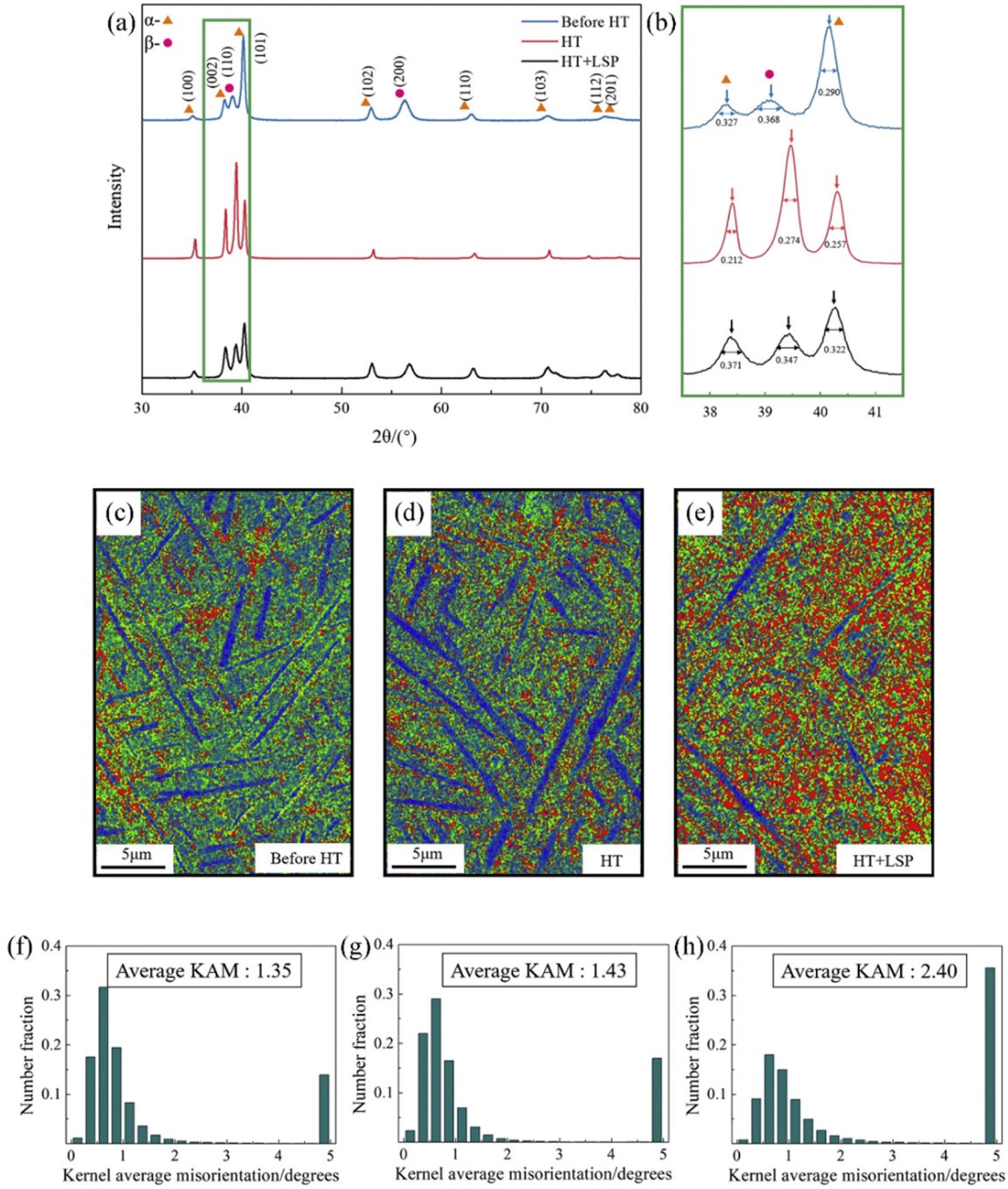


**Fig. 12** XRD patterns of WAAM part (a, b); KAM maps for samples without heat treatment (HT) (c), with HT (d) and with HT+LSP (e); KAM charts for samples without HT (f), with HT (g) and with HT+LSP (h) [140]

depth of several millimeters. Residual stress is partially released in this region [148].

YANG et al [149] found that interlayer UIT forms a "bamboo-like" structure [150]. This results from the superposition of "epitaxial grain growth" [151−153] and UIT. The average size of columnar crystals before UIT treatment was 785 μm. After UIT treatment, the average lengths of short columnar and equiaxed crystals were 371 and 186 μm, respectively. WANG et al [154] found that UIT reduces the average grain size from 420 to 280 μm.

UIT can reduce the tensile stress generated during solidification [155]. WALKER et al [156] pointed out that the higher the residual compressive stress, the better the life and fatigue resistance of the part. GAO et al [157] found that ultrasonic can make stress distribution more uniform. ZHOU

et al [158] established a UIT FEA model, and the results showed that UIT can produce a compressive stress layer of about 4 mm on the material surface, as shown in Fig. 13. Further, they studied the magnitude and direction of the principal stress and principal shear stress and analyzed the plastic deformation behavior of the specimen during UIT process. They found that the order of plastic slip in the plastic deformation zone is inconsistent with the direction of compressive stress (Figs. 13(a−c)). As a result, curved fibrous tissue is formed in the sample, which is thought to help reduce inherent defects such as porosity and cracks, improve performance and play an important role in densification of metal WAAM components.

UIT can improve the mechanical properties of materials. WANG and SHI [154] found that the microstructure and anisotropy of the specimens are improved after UIT. HE et al [159] found that UIT can enhance the mechanical properties and improve the anisotropy of WAAM titanium alloy parts. After UIT, the horizontal tensile strength increases by 5.1%, and the vertical direction increases by 12.5%. CHEN et al [160] found that the fatigue strength of the 7A52 aluminum alloy welded joint increases by 32.33% after UIT. ZHANG et al [161] and LI et al [162] found that UIT can change the preferred orientation of materials to ⟨111⟩. SONG et al [163] used UIT after SLM and found that UIT can effectively reduce porosity. LESYK et al [164] found that after UIT treatment, the surface roughness and porosity are reduced, and the microhardness is improved.

### 5.3 Hybrid additive−subtractive manufacturing

WAAM is limited in industrial applications due to poor molding accuracy and surface quality, and large residual stress. To solve these problems, some researchers combine additive manufacturing with subtractive manufacturing. The traditional subtractive manufacturing, such as milling, can improve surface quality and size accuracy [165]. At the same time, removing materials can cause the release and redistribution of initial residual stress. These are believed to improve the performance of WAAM components.

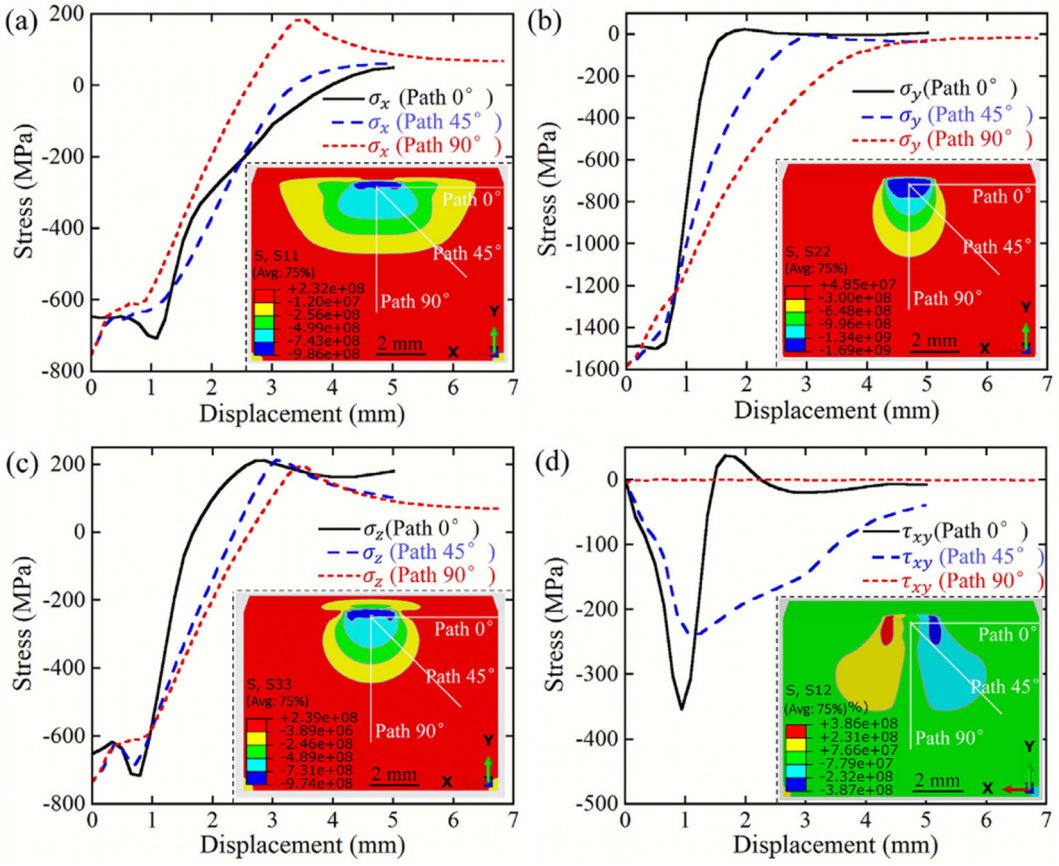


**Fig. 13** Finite element model of residual stress distribution in 304 stainless steel after UIT treatment in different directions [158]: (a) $\sigma_x$; (b) $\sigma_y$; (c) $\sigma_z$; (d) $\tau_{xy}$

Figure 14(a) shows the hybrid additive−subtractive manufacturing (HASM) equipment composed of WAAM and milling robot systems. The control cabinets of the two robots communicate through explicit collaboration, enabling the integration of WAAM and the milling process. In HSAM, additive manufacturing (AM) and subtractive manufacturing (SM) are carried out alternately [166], as shown in Fig. 14(c). Compared to traditional SM, HASM can reduce engineering and material costs, making it more economically attractive for more expensive and harder-to-process materials [167].

Subtractive manufacturing has been widely used after AM, which is necessary to improve the surface finish of the parts. DU et al [168,169] studied the composite manufacturing of reduced material manufacturing (SM) and SLM, as shown in Fig. 15(a). SM process is added after several layers are deposited, and the addition and subtraction processes alternate until the part is complete. This manufacturing method allows for complex internal structures such as cooling water channels and deep grooves. After SM, the dimensional and geometric errors generated in AM can be greatly reduced, as shown in Figs. 15(b, c). KARUNAKARAN et al [95] introduced milling to arc welding and dramatically enhanced the forming accuracy of the finished parts. SONG et al [170−172] combined WAAM with milling, improving the surface topography of the parts significantly.

SM can improve the stress distribution in the forming parts, and transform the harmful tensile stress into compressive stress, thus reducing the deformation and increasing fatigue strength [173]. It is worth noting that the stress redistribution caused by SM may lead to secondary deformation, thus affecting dimensional accuracy and assembly accuracy [166]. SUNNY et al [174] studied the influence of initial residual stress on machining stress and deformation, and the results showed that

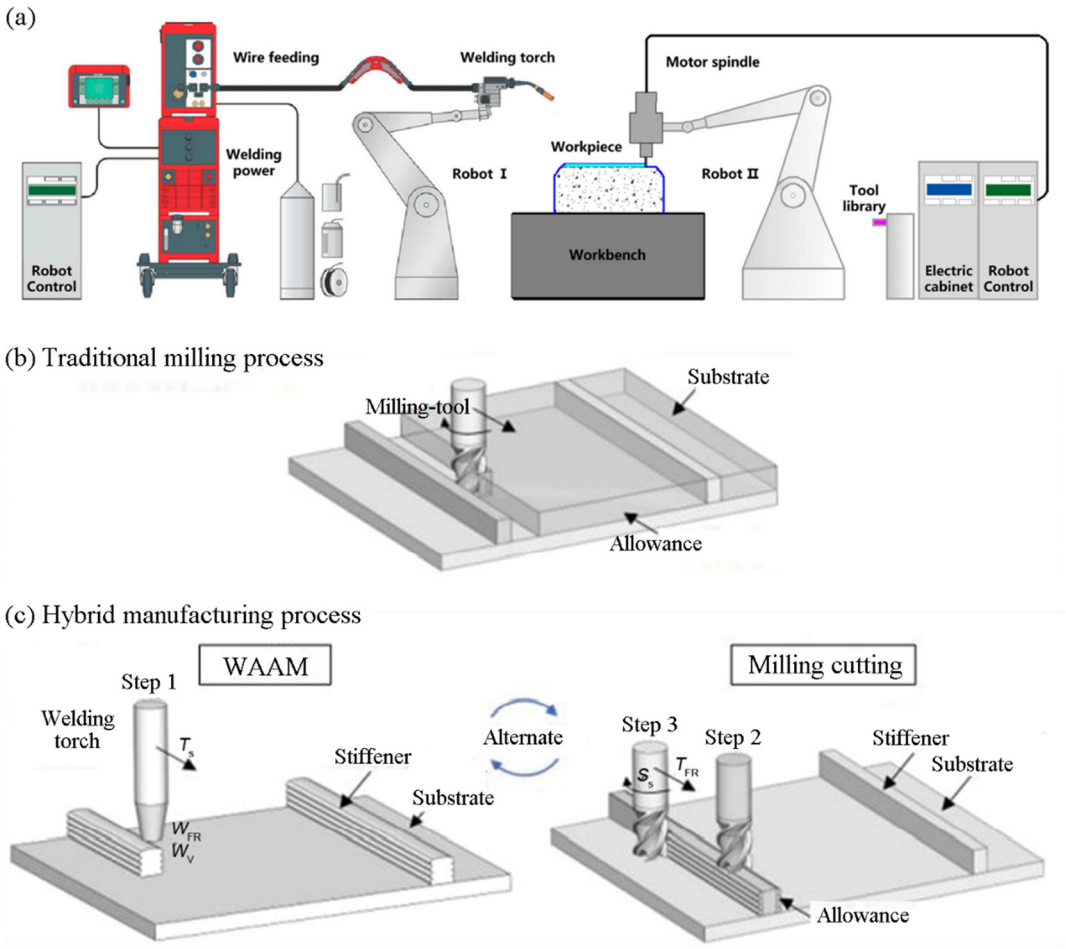


**Fig. 14** Schematic diagram of additive and subtractive composite manufacturing equipment [165] (a); Schematic diagram of thin-walled parts manufactured by traditional milling (b); Schematic diagram of thin-walled parts manufactured by additive and subtractive composite manufacturing [166] (c)

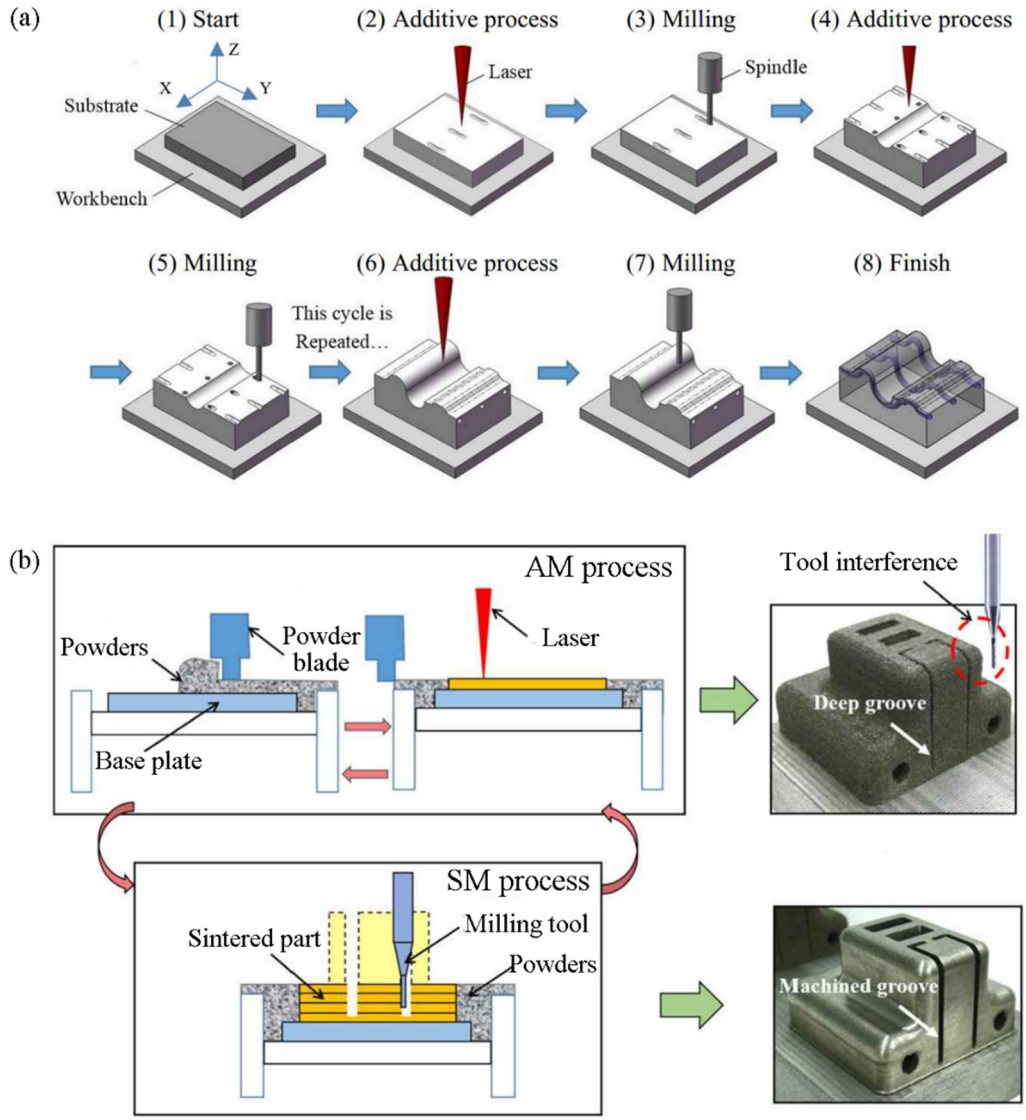


**Fig. 15** Schematic diagram of SM/SLM composite manufacturing process [168] (a); SM/AM composite manufacturing diagram and improvement of surface quality of parts [168] (b)

the initial residual stress can affect the improvement effect of the SM process. SALONITIS et al [175] came to similar conclusions. Through numerical simulations of HASM, they found that the ability of SM to correct the deformation of parts is limited when the initial residual stress is enormous.

## 6 Summary

(1) In the pre-treatment, numerical simulation technology can greatly simplify the experimental work of WAAM and provide guidance for the research direction. Excellent slicing software and path planning can also improve the quality of WAAM parts.

(2) In the WAAM process, proper parameters are also the key to ensuring the quality of parts. Factors such as temperature, arc and droplet need to be monitored to ensure stability during surfacing. Morphology control is the premise of WAAM. The process parameters have a great influence on the morphology. The microstructures of different parts of the molten pool are different with different technological parameters. Therefore, the quality of WAAM parts can be improved only by clarifying the influence law of process parameters on the performance of WAAM parts. In addition, because WAAM is an unstable process, on-line monitoring and control system is essential, which is of great significance to improving the quality of WAAM parts.

(3) Post-treatment is usually used to reduce

residual stress and deformation. Standard post-treatment methods include rolling, impact strengthening and milling. The macroscopic characteristics, microstructure and mechanical properties of the component are controlled by plastic deformation in additive manufacturing. The stability of hot rolling deformation process is poor. Cold rolling is not suitable for stronger metals. Surface treatment has a limited effect on micro-structure, but it is effective to redistribute and transform residual stress. Milling can improve the surface quality of WAAM parts and the residual stress, but the effect is insignificant when the initial residual stress is large.

## Acknowledgments

The authors acknowledge financial supports from the National Natural Science Foundation of China (Nos. 52075250, 52175468), the China Postdoctoral Science Foundation (No. 2020M683376), State Key Laboratory of Advanced Welding and Joining, Harbin Institute of Technology, China (No. AWJ-22M13), and the Fundamental Research Funds for the Central Universities, China (No. NT2021018).

## References

[1] ALCISTO J, ENRIQUEZ A, GARCIA H, HINKSON S, STEELMAN T, SILVERMAN E, VALDOVINO P, GIGERENZER H, FOYOS J, OGREN J, DOREY J, KARG K, MCDONALD T, ES-SAID O S. Tensile properties and microstructures of laser-formed Ti−6Al−4V [J]. Journal of Materials Engineering and Performance, 2011, 20(2): 203−212.

[2] TOFAIL S A M, KOUMOULOS E P, BANDYOPADHYAY A, BOSE S , O'DONOGHUE L, CHARITIDIS C. Additive manufacturing: Scientific and technological challenges, market uptake and opportunities [J]. Materials Today, 2018, 21(1): 22−37.

[3] FRAZIER W E. Metal additive manufacturing: A review [J]. Journal of Materials Engineering and Performance, 2014, 23(6): 1917−1928.

[4] SHI Xue-zhi, MA Shu-yuan, LIU Chang-meng, WU Qian-ru, LU Ji-ping LIU Yu-de, SHI Wen-tian. Selective laser melting-wire arc additive manufacturing hybrid fabrication of Ti−6Al−4V alloy: Microstructure and mechanical properties [J]. Materials Science and Engineering A, 2017, 684: 196−204.

[5] LEE Jian-yuan, NAGALINGAM A P, YEO S H. A review on the state-of-the-art of surface finishing processes and related ISO/ASTM standards for metal additive manufactured components [J]. Virtual and Physical Prototyping, 2021, 16(1): 68−96.

[6] WANG Pei, ECKERT J, PRASHANTH K G, WU Ming-wei, KABAN I, XI Li-xia, SCUDINO S. A review of particulate-reinforced aluminum matrix composites fabricated by selective laser melting [J]. Transactions of Nonferrous Metals Society of China, 2020, 30(8): 2001−2034.

[7] HAN Li-ying, WANG Cun-shan. Microstructure and properties of $Ti_{64.51}Fe_{26.40}Zr_{5.86}Sn_{2.93}Y_{0.30}$ biomedical alloy fabricated by laser additive manufacturing [J]. Transactions of Nonferrous Metals Society of China, 2020, 30(12): 3274−3286.

[8] WEN Yao-jie, ZHANG Bai-cheng, LIU Shu-ying, CAI Wei, WANG Pei, LEE C J J, MA Jun-da, QU Xuan-hui. A novel experimental method for in situ strain measurement during selective laser melting [J]. Virtual and Physical Prototyping, 2020, 15(Sup1): 583−595.

[9] FU Peng-huai, WANG Nan-qing, LIAO Hai-guang, XU Wen-yu, PENG Li-ming, CHEN Juan, HU Guo-qi, DING Wen-jiang. Microstructure and mechanical properties of high strength Mg−15Gd−1Zn−0.4Zr alloy additive-manufactured by selective laser melting process [J]. Transactions of Nonferrous Metals Society of China, 2021, 31(7): 1969−1978.

[10] LIU Tian-yu, MIN Xiao-hua, ZHANG Shuang, WANG Cun-shan, DONG Chuang. Microstructures and mechanical properties of Ti−Al−V−Nb alloys with cluster formula manufactured by laser additive manufacturing [J]. Transactions of Nonferrous Metals Society of China, 2021, 31(10): 3012−3023.

[11] LEE K H, YUN Gun-jin. A novel heat source model for analysis of melt pool evolution in selective laser melting process [J]. Additive Manufacturing, 2020, 36: 101497.

[12] YAP C Y, CHUA C K, DONG Zhi-li, LIU Zhong-hong, ZHANG Dan-qing, LOH L E, SING S L. Review of selective laser melting: Materials and applications [J]. Applied Physics Reviews, 2015, 2(4): 041101.

[13] GAJAPATHI S S, MITRA S K, MENDEZ P F. Controlling heat transfer in micro electron beam welding using volumetric heating [J]. International Journal of Heat and Mass Transfer, 2011, 54(25/26): 5545−5553.

[14] RAGHAVAN N, DEHOFF R, PANNALA S, SIMUNOVIC S, KIRKA M, TURNER J, CARLSON N, BABU S S. Numerical modeling of heat-transfer and the influence of process parameters on tailoring the grain morphology of IN718 in electron beam additive manufacturing [J]. Acta Materialia, 2016, 112: 303−314.

[15] EDWARDS P, O'CONNER A, RAMULU M. Electron beam additive manufacturing of titanium components: Properties and performance [J]. Journal of Manufacturing Science and Engineering, 2013, 135(6): 061016.

[16] ZIĘTALA M, DUREJKO T, PANOWICZ R, KONARZEWSKI M. Microstructure evolution of 316L steel prepared with the use of additive and conventional methods and subjected to dynamic loads: A comparative study [J]. Materials, 2020, 13(21): 4893.

[17] SHU Xi, CHEN Guo-qing, LIU Jun-peng, ZHANG Bing-gang, FENG Ji-cai. Microstructure evolution of copper/steel gradient deposition prepared using electron beam freeform fabrication [J]. Materials Letters, 2018, 213: 374−377.

[18] XU Jun-qiang, ZHU Jun, FAN Ji-kang, ZHOU Qi, PENG

Yong, GUO Shun. Microstructure and mechanical properties of Ti−6Al−4V alloy fabricated using electron beam freeform fabrication [J]. Vacuum, 2019, 167: 364−373.

[19] SLOTWINSKI J A, GARBOCZI E J, HEBENSTREIT K M. Porosity measurements and analysis for metal additive manufacturing process control [J]. Journal of Research of the National Institute of Standards and Technology, 2014, 119: 494−528.

[20] XIA Chun-yang, PAN Zeng-xi, POLDEN J, LI Hui-jun, XU Yang-ling, CHEN Shan-ben, ZHANG Yu-ming. A review on wire arc additive manufacturing: Monitoring, control and a framework of automated system [J]. Journal of Manufacturing Systems, 2020, 57: 31−45.

[21] LIU Jie-nan, XU Yan-ling, GE Yu, HOU Zhen, CHEN Shan-ben. Wire and arc additive manufacturing of metal components: a review of recent research developments [J]. The International Journal of Advanced Manufacturing Technology, 2020, 111(1): 149−198.

[22] POQUILLON D, ARMAND C, HUEZ J. Oxidation and oxygen diffusion in Ti−6Al−4V alloy: Improving measurements during Sims analysis by rotating the sample [J]. Oxidation of Metals, 2013, 79(3): 249−259.

[23] YUE Li-yang, WANG Zeng-bo, LI Lin. Material morphological characteristics in laser ablation of alpha case from titanium alloy [J]. Applied Surface Science, 2012, 258(20): 8065−8071.

[24] HAUSER T, REISCH R T, BREESE P P, NALAM Y, JOSHI K S, BELA K, KAMPS T, VOLPP J, KAPLAN A F H. Oxidation in wire arc additive manufacturing of aluminium alloys [J]. Additive Manufacturing, 2021, 41: 101958.

[25] LANGELANDSVIK G, ERIKSSON M, AKSELSEN O M, ROVEN H J. Wire arc additive manufacturing of AA5183 with TiC nanoparticles [J]. The International Journal of Advanced Manufacturing Technology, 2022, 119(1): 1047−1058.

[26] MUGHAL M P, FAWAD H, MUFTI R A. Three-dimensional finite-element modelling of deformation in weld-based rapid prototyping [J]. Proceedings of the Institution of Mechanical Engineers, Part C: Journal of Mechanical Engineering Science, 2006, 220(6): 875−885.

[27] HU Tao, GUO Chun, HE Zi-liang,WEI Bao-li, CHEN Feng. Current status of arc additive manufacturing technology [J]. Mechanical and Electronic Information, 2020(5): 98−99. (in Chinese)

[28] STRANO G, HAO Liang, EVERSON R M, EVANS K E. Surface roughness analysis, modelling and prediction in selective laser melting [J]. Journal of Materials Processing Technology, 2013, 213(4): 589−597.

[29] CHERNOVOL N, SHARMA A, TJAHJOWIDODO T, LAUWERS B, RYMENANT P V. Machinability of wire and arc additive manufactured components [J]. CIRP Journal of Manufacturing Science and Technology, 2021, 35: 379−389.

[30] MA Chi, LIU Yong-hong, JIN Hui. The optimization for shape control in wire and arc additive manufacturing [J]. Electromachining & Mould, 2020(2): 61−64. (in Chinese)

[31] RAFIEAZAD M, GHAFFARI M, NEMANI A V, NASIRI A. Microstructural evolution and mechanical properties of a low-carbon low-alloy steel produced by wire arc additive manufacturing [J]. The International Journal of Advanced Manufacturing Technology, 2019, 105(5): 2121−2134.

[32] ZHOU Ying-hui, LIN Xin, KANG Nan, TANG Yao, HUANG Wei-dong, WANG Zhen-nan. The heterogeneous band microstructure and mechanical performance in a wire + arc additively manufactured 2219 Al alloy [J]. Additive Manufacturing, 2022, 49: 102486.

[33] WANG Chang-ji, LIU Tie-gang, ZHU Ping, LU Yong-hao, SHOJI T. Study on microstructure and tensile properties of 316L stainless steel fabricated by CMT wire and arc additive manufacturing [J]. Materials Science and Engineering A, 2020, 796: 140006.

[34] BAI Jiu-yang, YANG Chun-li, LIN San-bao, DONG Bo-lun, FAN Cheng-lei. Mechanical properties of 2219-Al components produced by additive manufacturing with TIG [J]. The International Journal of Advanced Manufacturing Technology, 2016, 86(1): 479−485.

[35] SUN Lai-bo, JIANG Feng-chun, HUANG Rui-sheng, YUAN Ding, GUO Chun-huan, WANG Jian-dong. Anisotropic mechanical properties and deformation behavior of low-carbon high-strength steel component fabricated by wire and arc additive manufacturing [J]. Materials Science and Engineering A, 2020, 787: 139514.

[36] YEHOROV Y, DA SILVA L J, SCOTTI A. Exploring the use of switchback for mitigating homoepitaxial unidirectional grain growth and porosity in WAAM of aluminium alloys [J]. The International Journal of Advanced Manufacturing Technology, 2019, 104(1): 1581−1592.

[37] SEOW C E, COULES H E, WU Gui-yi, KHAN R H U, XU Xiang-fang WILLIAMS S. Wire + arc additively manufactured Inconel 718: Effect of post-deposition heat treatments on microstructure and tensile properties [J]. Materials & Design, 2019, 183: 108157.

[38] BABY J, AMIRTHALINGAM M. Microstructural development during wire arc additive manufacturing of copper-based components [J]. Welding in the World, 2020, 64(2): 395−405.

[39] YU Jun, QIN Tou, LIN Xin, WANG Jun-jie, ZHANG Yu-feng, WANG Shi-yao, YANG Jing-yi, HUANG Wei-dong. Electrochemical dissolution and passivation of laser additive manufactured Ti6Al4V controlled by elements segregation and phases distribution [J]. Transactions of Nonferrous Metals Society of China, 2021, 31(12): 3739−3751.

[40] LAGHI V, TONELLI L, PALERMO M, BRUGGI M, SOLA R, CESCHINI L, TROMBETTI T. Experimentally-validated orthotropic elastic model for wire-and-arc additively manufactured stainless steel [J]. Additive Manufacturing, 2021, 42: 101999.

[41] SEOW C E, ZHANG Jie, COULES H E, WU Gui-yi, JONES C, DING Jia-luo, WILLIAMS S. Effect of crack-like defects on the fracture behaviour of wire + arc additively manufactured nickel-base alloy 718 [J]. Additive Manufacturing, 2020, 36: 101578.

[42] HASSEL T, CARSTENSEN T. Properties and anisotropy behaviour of a nickel base alloy material produced by robot-based wire and arc additive manufacturing [J]. Welding in the World, 2020, 64(11): 1921−1931.

[43] GU Jiang-long, GAO Min-jie, YANG Shuo-jiang, BAI Jing, ZHAI Yu-chun, DING Jia-luo. Microstructure, defects, and mechanical properties of wire + arc additively manufactured

AlCu4.3−Mg1.5 alloy [J]. Materials & Design, 2020, 186: 108357.

[44] WU Qian-ru, MUKHERJEE T, LIU Chang-meng, LU Ji-ping, DEBROY T. Residual stresses and distortion in the patterned printing of titanium and nickel alloys [J]. Additive Manufacturing, 2019, 29: 100808.

[45] CHIN R K, BEUTH J L, AMON C H. Thermomechanical modeling of successive material deposition in layered manufacturing [C]//International Solid Freeform Fabrication Symposium. Texas, UAS: University of Texas at Austin, 1996.

[46] BEUTH J L, NARAYAN S H. Residual stress-driven delamination in deposited multi-layers [J]. International Journal of Solids and Structures, 1996, 33(1): 65−78.

[47] GENG Ru-wei, DU Jun, WEI Zheng-ying. Research progress in formation law, microstructure evolution and residual stress in wire and arc additive manufacturing [J]. Materials for Mechanical Engineering, 2020, 44(12): 11−17. (in Chinese)

[48] SAMES W J, LIST F A, PANNALA S, DEHOFF R R, BABU S S. The metallurgy and processing science of metal additive manufacturing [J]. International Materials Reviews, 2016, 61(5): 315−360

[49] CHEN Xi, KONG Fan-rong, FU You-heng, ZHAO Xu-shan, LI Run-sheng, WANG Gui-lan, ZHANG Hai-ou. A review on wire-arc additive manufacturing: Typical defects, detection approaches, and multisensor data fusion-based model [J]. The International Journal of Advanced Manufacturing Technology, 2021, 117(3): 707−727.

[50] YIN Bo, MA Hong-wei, WANG Jing-biao, FANG Kun, ZHAO Hong, LIU Yun-feng. Effect of CaF2 addition on macro/microstructures and mechanical properties of wire and arc additive manufactured Ti−6Al−4V components [J]. Materials Letters, 2017, 190: 64−66.

[51] WANG Yan-hu, CHEN Xi-zhang, KONOVALOV S V. Additive manufacturing based on welding arc: A low-cost method [J]. Journal of Surface Investigation: X-ray, Synchrotron and Neutron Techniques, 2017, 11(6): 1317−1328.

[52] WANG Yi-peng, QI Bo-jin, CONG Bao-qiang, YANG Ming-xuan, LIU Fang-jun. Arc characteristics in double-pulsed VP-GTAW for aluminum alloy [J]. Journal of Materials Processing Technology, 2017, 249: 89−95.

[53] GU Jiang-long, DING Jia-luo, WILLIAMS S W, GU Hui-min, MA Pei-hua, ZHAI Yu-chun. The effect of inter-layer cold working and post-deposition heat treatment on porosity in additively manufactured aluminum alloys [J]. Journal of Materials Processing Technology, 2016, 230: 26−34.

[54] LONG Ping, WEN Dongxu, MIN Jie, ZHENG Zhi-zhen, LI Jian-jun, LIU Yan-xing. Microstructure evolution and mechanical properties of a wire-arc additive manufactured austenitic stainless steel: Effect of processing parameter [J]. Materials, 2021, 14(7): 1681.

[55] BAI Jiu-yang, FAN Cheng-lei, LIN San-bao, YANG Chun-li, DONG Bo-lun. Mechanical properties and fracture behaviors of GTA-additive manufactured 2219-Al after an especial heat treatment [J]. Journal of Materials Engineering and Performance, 2017, 26(4): 1808−1816.

[56] LI Rui-di, NIU Peng-da, YUAN Tie-chui, LI Zhi-ming. Displacive transformation as pathway to prevent micro-cracks induced by thermal stress in additively manufactured strong and ductile high-entropy alloys [J]. Transactions of Nonferrous Metals Society of China, 2021, 31(4): 1059−1073.

[57] ERMAKOVA A, MEHMANPARAST A, GANGULY S, RAZAVI J, BERTO F. Fatigue crack growth behaviour of wire and arc additively manufactured ER70S-6 low carbon steel components [J]. International Journal of Fracture, 2021: 1−13.

[58] YAO Xin-xin, LI Jian-yu, WANG Yi-fei, GAO Xiang, ZHANG Zhao. Numerical simulation of powder effect on solidification in directed energy deposition additive manufacturing [J]. Transactions of Nonferrous Metals Society of China, 2021, 31(9): 2871−2884.

[59] PRAJADHIANA K P, MANURUNG Y H P, ADENAN M S, MOHAMED M A, BAUER A. Experimental verification of numerical computation with evolved material property model and sensitivity analysis on WAAM distortion using P-GMAW [J]. Arabian Journal for Science and Engineering, 2021, 46(12): 12525−12536.

[60] SUN Jia-min, HENSEL J, KÖHLER M, DILGER K. Residual stress in wire and arc additively manufactured aluminum components [J]. Journal of Manufacturing Processes, 2021, 65: 97−111.

[61] ABBASZADEH M, HÖNNIGE J R, MARTINA F, NETO L, KASHAEV N, COLEGROVE P, WILLIAMS S, KLUSEMANN B. Numerical investigation of the effect of rolling on the localized stress and strain induction for wire + arc additive manufactured structures [J]. Journal of Materials Engineering and Performance, 2019, 28(8): 4931−4942.

[62] DING Dong-hong, ZHANG Shi-min, LU Qiang-hua, PAN Zeng-xi, LI Hui-jun, WANG Kai. The well-distributed volumetric heat source model for numerical simulation of wire arc additive manufacturing process [J]. Materials Today Communications, 2021, 27: 102430.

[63] ABE T, KANEKO J, SASAHARA H. Thermal sensing and heat input control for thin-walled structure building based on numerical simulation for wire and arc additive manufacturing [J]. Additive Manufacturing, 2020, 35: 101357.

[64] HUANG Hui, MA Nin-shu, CHEN Jian, FENG Zhi-li, MURAKAWA H. Toward large-scale simulation of residual stress and distortion in wire and arc additive manufacturing [J]. Additive Manufacturing, 2020, 34: 101248.

[65] HUANG Jian-kang, GUAN Zhi-chen, YU Shu-hong, YU Xiao-quan, YUAN Wen, LI Nan, FAN Ding. A 3D dynamic analysis of different depositing processes used in wire arc additive manufacturing [J]. Materials Today Communications, 2020, 24: 101255.

[66] GORNYAKOV V, SUN Yong-le, DING Jia-luo, WILLIAMS S. Computationally efficient models of high pressure rolling for wire arc additively manufactured components [J]. Applied Sciences, 2021, 11(1): 402.

[67] CADIOU S, COURTOIS M, CARIN M, BERCKMANS W, MASSON P L. 3D heat transfer, fluid flow and electromagnetic model for cold metal transfer wire arc additive manufacturing (Cmt-Waam) [J]. Additive

Manufacturing, 2020, 36: 101541.

[68] HEJRIPOUR F, VALENTINE D T, AIDUN D K. Study of mass transport in cold wire deposition for Wire Arc Additive Manufacturing [J]. International Journal of Heat and Mass Transfer, 2018, 125: 471−484.

[69] SAADATMAND M, TALEMI R. Study on the thermal cycle of wire arc additive manufactured (WAAM) carbon steel wall using numerical simulation [J]. Frattura ed Integrità Strutturale, 2020, 14(52): 98−104.

[70] LI Rong, XIONG Jun. Influence of interlayer dwell time on stress field of thin-walled components in WAAM via numerical simulation and experimental tests [J]. Rapid Prototyping Journal, 2019, 25(8): 1433−1441.

[71] HACKENHAAR W, MAZZAFERRO J A E, MONTEVECCHI F, CAMPATELLI G. An experimental−numerical study of active cooling in wire arc additive manufacturing [J]. Journal of Manufacturing Processes, 2020, 52: 58−65.

[72] OYAMA K, DIPLAS S, M'HAMDI M, GUNNÆS A E, AZAR A S. Heat source management in wire-arc additive manufacturing process for Al−Mg and Al−Si alloys [J]. Additive Manufacturing, 2019, 26: 180−192.

[73] ZHANG Jian-sheng, ZHOU Jie, WANG Qiu-yun, XIAO Gui-qian, QUAN Guo-zheng. Process planning of automatic wire arc additive remanufacturing for hot forging die [J]. The International Journal of Advanced Manufacturing Technology, 2020, 109(5): 1613−1623.

[74] WANG Su, WANG Yan, CHEN Chin-sheng, Zhu Xin-xiong. An adaptive slicing algorithm and data format for functionally graded material objects [J]. The International Journal of Advanced Manufacturing Technology, 2013, 65(1): 251−258.

[75] DING Dong-hong, PAN Zeng-xi, CUIURI D, LI Hui-jun. Process planning for robotic wire and arc additive manufacturing [C]//IEEE 10th Conference on Industrial Electronics and Applications (ICIEA). LEEE, 2015: 2000−2003.

[76] WANG Xiao-long, WANG Ai-min, LI Yue-bo. A sequential path-planning methodology for wire and arc additive manufacturing based on a water-pouring rule [J]. The International Journal of Advanced Manufacturing Technology, 2019, 103(9): 3813−3830.

[77] ZHAO Yun, LI Fang, CHEN Shu-jun, LU Zhen-yang. Unit block–based process planning strategy of WAAM for complex shell–shaped component [J]. The International Journal of Advanced Manufacturing Technology, 2019, 104(9): 3915−3927.

[78] REBAIOLI L, MAGNONI P, FASSI I, PEDROCCHI N, TOSATTI L M. Process parameters tuning and online re-slicing for robotized additive manufacturing of big plastic objects [J]. Robotics and Computer−Integrated Manufacturing, 2019, 55: 55−64.

[79] ZHANG Lian-chong. Research on slicing and path planning of robot welding rapid remanufacturing forming [D]. Urumqi: Xinjiang University, 2013. (in Chinese)

[80] SCHMITZ M, WIARTALLA J, GELFGREN M, MANN S, CORVES B, HÜSING M. A Robot-centered path-planning algorithm for multidirectional additive manufacturing for WAAM processes and pure object manipulation [J]. Applied Sciences, 2021, 11(13): 5759.

[81] DING Dong-hong, PAN Zeng-xi, CUIURI D, LI Hui-jun, LARKIN N. Adaptive path planning for wire-feed additive manufacturing using medial axis transformation [J]. Journal of Cleaner Production, 2016, 133: 942−952.

[82] DIOURTÉ A, BUGARIN F, BORDREUIL C, SEGONDS S. Continuous three-dimensional path planning (CTPP) for complex thin parts with wire arc additive manufacturing [J]. Additive Manufacturing, 2021, 37: 101622.

[83] FENG Guang-lei, LIU Bin, CHEN Hui-hui. Compound-filled path generation and optimization for FDM [J]. Computer Engineering & Science, 2017, 39(6): 1149−1154. (in Chinese)

[84] VERMA D, DONG Yu, SHARMA M, CHAUDHARY A K. Advanced processing of 3D printed biocomposite materials using artificial intelligence [J]. Materials and Manufacturing Processes, 2022, 37(5): 518−538.

[85] LIU Bing, SHEN Hong-yao, ZHOU Ze-yu, JIN Jia-ao, FU Jian-zhong. Research on support-free WAAM based on surface/interior separation and surface segmentation [J]. Journal of Materials Processing Technology, 2021, 297: 117240.

[86] DAI Fu-sheng, ZHANG Shuai-feng, LI Run-sheng, ZHANG Hai-ou. Multiaxis wire and arc additive manufacturing for overhangs based on conical substrates [J]. Rapid Prototyping Journal, 2021, 28(1): 126−142

[87] KUMAR S, SHAHI A S. Effect of heat input on the microstructure and mechanical properties of gas tungsten arc welded AISI 304 stainless steel joints [J]. Materials & Design, 2011, 32(6): 3617−3623.

[88] XIONG Jun, ZHANG Guang-jun, ZHANG Wei-hua. Forming appearance analysis in multi-layer single-pass GMAW-based additive manufacturing [J]. The International Journal of Advanced Manufacturing Technology, 2015, 80(9): 1767−1776.

[89] XIONG Yi-bo, WEN Dong-xu, ZHENG Zhi-zhen, LI Jian-jun. Effect of interlayer temperature on microstructure evolution and mechanical performance of wire arc additive manufactured 300M steel [J]. Materials Science and Engineering A, 2022, 831: 142351.

[90] WEN Dong-xu, LONG Ping, LI Jian-jun, HUANG Liang, ZHENG Zhi-zeng. Effects of linear heat input on microstructure and corrosion behavior of an austenitic stainless steel processed by wire arc additive manufacturing [J]. Vacuum, 2020, 173: 109131.

[91] DINOVITZER M, CHEN X, LALIBERTE J, HUANG Xiao, FREI H. Effect of wire and arc additive manufacturing (WAAM) process parameters on bead geometry and microstructure [J]. Additive Manufacturing, 2019, 26: 138−146.

[92] KLEIN T, SCHNALL M. Control of macro-/microstructure and mechanical properties of a wire-arc additive manufactured aluminum alloy [J]. The International Journal of Advanced Manufacturing Technology, 2020, 108(1): 235−244.

[93] MICHALERIS P. Modeling metal deposition in heat transfer analyses of additive manufacturing processes [J]. Finite Elements in Analysis and Design, 2014, 86: 51−60.

[94] WU Bin-tao, PAN Zeng-xi, DING Dong-hong, CUIURI D,

LI Hui-jun, FEI Zhen-yu. The effects of forced interpass cooling on the material properties of wire arc additively manufactured Ti6Al4V alloy [J]. Journal of Materials Processing Technology, 2018, 258: 97−105.

[95] KARUNAKARAN K P, SURYAKUMAR S, PUSHPA V, AKULA S. Low cost integration of additive and subtractive processes for hybrid layered manufacturing [J]. Robotics and Computer−Integrated Manufacturing, 2010, 26(5): 490−499.

[96] LI Fang, CHEN Shu-jun, SHI Jun-biao, ZHAO Yun, TIAN Hong-yu. Thermoelectric cooling-aided bead geometry regulation in wire and arc-based additive manufacturing of thin-walled structures [J]. Applied Sciences, 2018, 8(2): 207.

[97] LIU Guang-chao, XIONG Jun. External filler wire based GMA-AM process of 2219 aluminum alloy [J]. Materials and Manufacturing Processes, 2020, 35(11): 1268−1277.

[98] HAN Qing-lin, GAO Jia, HAN Chang-le, ZHANG Guang-jun, LI Yong-zhe. Experimental investigation on improving the deposition rate of gas metal arc-based additive manufacturing by auxiliary wire feeding method [J]. Welding in the World, 2021, 65(1): 35−45.

[99] GU Jiang-long, WANG Xiao-shu, BAI Jing, DING Jia-luo, WILLIAMS S, ZHAI Yu-chun, LIU Kun. Deformation microstructures and strengthening mechanisms for the wire+arc additively manufactured Al−Mg4.5Mn alloy with inter-layer rolling [J]. Materials Science and Engineering A, 2018, 712: 292−301.

[100] DAI Dong-hua, GU Dong-dong, ZHANG Han, XIONG Jia-peng, MA Cheng-long, HONG Chen, POPRAWE R. Influence of scan strategy and molten pool configuration on microstructures and tensile properties of selective laser melting additive manufactured aluminum based parts [J]. Optics & Laser Technology, 2018, 99: 91−100.

[101] ZHANG Bo-wen, ZHANG Lai-qi. Research progress of AC cold metal transfer technology (advanced CMT) and its application in additive manufacturing [J]. Journal of New Industrialization, 2017, 7(11): 82−88. (in Chinese)

[102] FENG Ji-cai, ZHANG Hong-tao, HE Peng. The CMT short-circuiting metal transfer process and its use in thin aluminium sheets welding [J]. Materials & Design, 2009, 30(5): 1850−1852.

[103] ALI Y, HENCKELL P, HILDEBRAND J, REIMANN J, BERGMANN J P, BARNIKOL-OETTLER S. Wire arc additive manufacturing of hot work tool steel with CMT process [J]. Journal of Materials Processing Technology, 2019, 269: 109−116.

[104] JIANG Qi, ZHANG Pei-suo, LIU Zhi-qiang, YU Zhi-shui, SHI Hai-chuan. Microstructure and tensile properties of arc additive manufacturing 4043 aluminum alloy thin-walled parts by CMT with addition of pulse [J]. Materials for Mechanical Engineering, 2020, 44(1): 57−61. (in Chinese)

[105] ELREFAEY A. Effectiveness of cold metal transfer process for welding 7075 aluminium alloys [J]. Science and Technology of Welding and Joining, 2015, 20(4): 280−285.

[106] POSCH G, CHLADIL K, CHLADIL H. Material properties of CMT—Metal additive manufactured duplex stainless steel blade-like geometries [J]. Welding in the World, 2017, 61(5): 873−882.

[107] CONG Bao-qiang, DING Jia-luo, WILLIAMS S. Effect of arc mode in cold metal transfer process on porosity of additively manufactured Al−6.3%Cu alloy [J]. The International Journal of Advanced Manufacturing Technology, 2015, 76(9): 1593−1606.

[108] XIONG Jun, ZHANG Yi-yang, PI Yu-peng. Control of deposition height in WAAM using visual inspection of previous and current layers [J]. Journal of Intelligent Manufacturing, 2021, 32(8): 2209−2217.

[109] ZHANG Zhi-fen, YU Huan-wei, LV Na, CHEN Shan-ben. Real-time defect detection in pulsed GTAW of Al alloys through on-line spectroscopy [J]. Journal of Materials Processing Technology, 2013, 213(7): 1146−1156.

[110] JIA Chuan-bao, WU Chuan-song, ZHANG Yu-ming. Sensing controlled pulse key-holing condition in plasma arc welding [J]. Transactions of Nonferrous Metals Society of china, 2009, 19(2): 341−346.

[111] PAL K, BHATTACHARYA S, PAL S K. Investigation on arc sound and metal transfer modes for on-line monitoring in pulsed gas metal arc welding [J]. Journal of Materials Processing Technology, 2010, 210(10): 1397−1410.

[112] SHEVCHIK S A, KENEL C, LEINENBACH C, WASMER K. Acoustic emission for in situ quality monitoring in additive manufacturing using spectral convolutional neural networks [J]. Additive Manufacturing, 2018, 21: 598−604.

[113] RIEDER H, DILLHÖFER A, SPIES M, BAMBERG J, HESS T. Online monitoring of additive manufacturing processes using ultrasound [C]//Proceedings of the 11th European Conference on Non-destructive Testing. Prague, Czech Republic: e-Journal of Nondestructive Testing, 2014: 2194−2201.

[114] MA Yu-yang, HU Zhen-lin, TANG Yun, MA Shi-xiang, CHU Yan-wu, LI Xin, LUO Wei, GUO Lian-bo, ZENG Xiao-yan, LU Yong-feng. Laser opto-ultrasonic dual detection for simultaneous compositional, structural, and stress analyses for wire + arc additive manufacturing [J]. Additive Manufacturing, 2020, 31: 100956.

[115] SUÁREZ A, ALDALUR E, VEIGA F, ARTAZA T, TABERNERO I, LAMIKIZ A. Wire arc additive manufacturing of an aeronautic fitting with different metal alloys: From the design to the part [J]. Journal of Manufacturing Processes, 2021, 64: 188−197.

[116] CHEN Xi, FU You-heng, KONG Fan-rong, LI Run-sheng, XIAO Yu, HU Jian-nan, ZHANG Hai-ou. An in-process multi-feature data fusion nondestructive testing approach for wire arc additive manufacturing [J]. Rapid Prototyping Journal, 2021, 28(3): 573−584.

[117] SAFARZADE A, SHARIFITABAR M, AFARANI M S. Effects of heat treatment on microstructure and mechanical properties of Inconel 625 alloy fabricated by wire arc additive manufacturing process [J]. Transactions of Nonferrous Metals Society of China, 2020, 30(11): 3016−3030.

[118] YANG Liu-qing, YANG Yan-qing. Deformed microstructure and texture of Ti6Al4V alloy [J]. Transactions of Nonferrous Metals Society of China, 2014, 24(10): 3103−3110.

[119] LI Ming-xiang, ZHANG Tao, YU Fei, LU Shi-hong. Research progress of metal arc additive manufacturing and its composite manufacturing technology [J]. Aeronautical Manufacturing Technology, 2019, 62(17): 14−21. (in Chinese)

[120] AMIRI M M, FERESHTEH-SANIEE F. Influence of roll speed difference on microstructure, texture and mechanical properties of 7075 aluminum plates produced via combined continuous casting and rolling process [J]. Transactions of Nonferrous Metals Society of China, 2021, 31(4): 901−912.

[121] WANG Kang, WEN Dong-xu, LI Jian-jun, ZHENG Zhi-zhen, XIONG Yi-bo. Hot deformation behaviors of low-alloyed ultrahigh strength steel 30CrMnSiNi2A: Microstructure evolution and constitutive modeling [J]. Materials Today Communications, 2021, 26: 102009.

[122] XIONG Yi-bo, WEN Dong-xu, LI Jian-jun, WANG Kang, ZHENG Zhi-zhen. High-temperature deformation characteristics and constitutive model of an ultrahigh strength steel [J]. Metals and Materials International, 2021, 27(10): 3945−3958.

[123] XIE Cheng, WU Sheng-chuan, YU Yu-kang, ZHANG Hai-ou, HU Ya-nan, ZHANG Ming-bo, WANG Gui-lan. Defect-correlated fatigue resistance of additively manufactured Al−Mg4.5Mn alloy with in situ micro-rolling [J]. Journal of Materials Processing Technology, 2021, 291: 117039.

[124] ZHANG Haiou, WANG Xiang-ping, WANG Gui-lan, ZHANG Yang. Hybrid direct manufacturing method of metallic parts using deposition and micro continuous rolling [J]. Rapid Prototyping Journal, 2013, 19(6): 387−394.

[125] SOKOLOV P, ALESHCHENKO A, KOSHMIN A, CHEVERIKIN V, PETROVSKIY P, TRAVYANOV A, SOVA A. Effect of hot rolling on structure and mechanical properties of Ti−6Al−4V alloy parts produced by direct laser deposition [J]. The International Journal of Advanced Manufacturing Technology, 2020, 107(3): 1595−1603.

[126] POPOVICH A, SUFIIAROV V, POLOZOV I, BORISOV E, MASAYLO D, ORIOV A. Microstructure and mechanical properties of additive manufactured copper alloy [J]. Materials Letters, 2016, 179: 38−41.

[127] OH W J, LEE W J, KIM M S, JEON J B, SHIM D S. Repairing additive-manufactured 316L stainless steel using direct energy deposition [J]. Optics & Laser Technology, 2019, 117: 6−17.

[128] QIU Xiang, TARIQ N U H, QI Lu, ZAN Yu-ning, WANG Yu-jiang, WANG Ji-qiang, DU Hao, XIONG Tian-ying. In-situ $Si_p$/A380 alloy nano/micro composite formation through cold spray additive manufacturing and subsequent hot rolling treatment: Microstructure and mechanical properties [J]. Journal of Alloys and Compounds, 2019, 780: 597−606.

[129] MA Chi, LIU Yong-hong, JI Ren-jie, LI Chang-long. Review of wire and arc additive manufacturing: Technology genre and prospect [J]. Electromachining & Mould, 2020(4): 1−11. (in Chinese)

[130] TANGESTANI R, FARRAHI G H, SHISHEGAR M, AGHCHEHKANDI B P, GANGULY G, MEHMANPARAST A. Effects of vertical and pinch rolling on residual stress distributions in wire and arc additively manufactured components [J]. Journal of Materials Engineering and Performance, 2020, 29(4): 2073−2084.

[131] MARINELLI G, MARTINA F, GANGULY S, WILLIAMS S. Grain refinement in an unalloyed tantalum structure by combining wire+Arc additive manufacturing and vertical cold rolling [J]. Additive Manufacturing, 2020, 32: 101009.

[132] DONOGHUE J, ANTONYSAMY A A, MARTINA F, COLEGROVE P A, WILLIAMS S W, PRANGNELL P B. The effectiveness of combining rolling deformation with wire–arc additive manufacture on $\beta$-grain refinement and texture modification in Ti−6Al−4V [J]. Materials Characterization, 2016, 114: 103−114.

[133] ZHANG Tao, LI Hui-gui, GONG Hai, DING Jia-luo, WU Yun-xin, DIAO Cheng-lei, ZHANG Xiao-yong, WILLIAMS S. Hybrid wire-arc additive manufacture and effect of rolling process on microstructure and tensile properties of Inconel 718 [J]. Journal of Materials Processing Technology, 2022, 299: 117361.

[134] HÖNNIGE J, SEOW C E, GANGULY S, XU Xiang-fang, CABEZA S, COULES H, WILLIAMS S. Study of residual stress and microstructural evolution in as-deposited and inter-pass rolled wire plus arc additively manufactured Inconel 718 alloy after ageing treatment [J]. Materials Science and Engineering A, 2021, 801: 140368.

[135] HÖNNIGE J R, COLEGROVE P A, GANGULY S, ELMER E, KABRA S, WILLIAMS S. Control of residual stress and distortion in aluminium wire + arc additive manufacture with rolling [J]. Additive Manufacturing, 2018, 22: 775−783.

[136] JU Hong-tao, XU Dong-sheng, SHAN Fei-hu, YANG Rui. Finite element simulation of hybrid manufacturing of Ti−6Al−4V by wire arc additive manufacturing and rolling [J]. Rare Metal Materials and Engineering, 2020, 49(3): 878−882.

[137] MONTROSS C S, WEI Tao, YE Lin, CLARK G, MAI Y. Laser shock processing and its effects on microstructure and properties of metal alloys: A review [J]. International Journal of Fatigue, 2002, 24(10): 1021−1036.

[138] LIAO Yi-liang, YE Chang, CHENG G J. A review: Warm laser shock peening and related laser processing technique [J]. Optics & Laser Technology, 2016, 78: 15−24.

[139] SUN Ru-jian, LI Liu-he, ZHU Ying, GUO Wei, PENG Peng, CONG Bao-qiang, SUN Jian-fei, CHE Zhi-gang, LI Bo, GUO Chao, LIU Lei. Microstructure, residual stress and tensile properties control of wire-arc additive manufactured 2319 aluminum alloy with laser shock peening [J]. Journal of Alloys and Compounds, 2018, 747: 255−265.

[140] CHI Jia-xuan, CAI Zhong-yi, WAN Zhan-dong, ZHANG Hong-qiang, CHEN Zhen-lin, LI Liu-he, LI Ying, PENG Peng, GUO Wei. Effects of heat treatment combined with laser shock peening on wire and arc additive manufactured Ti17 titanium alloy: Microstructures, residual stress and mechanical properties [J]. Surface and Coatings Technology, 2020, 396: 125908.

[141] NIE Xiang-fan, HE Wei-feng, ZHOU Liu-cheng, LI Qi-peng, WANG Xue-de. Experiment investigation of laser shock peening on TC6 titanium alloy to improve high cycle fatigue performance [J]. Materials Science and Engineering A, 2014, 594: 161−167.

[142] ROY S, SARKAR A, SUWAS S. On characterization of deformation microstructure in Boron modified Ti−6Al−4V alloy [J]. Materials Science and Engineering A, 2010, 528(1): 449−458.

[143] SUN Ru-jian, ZHU Ying, LI Liu-he, GUO Wei, PENG Peng. Effect of laser shock peening on microstructure and residual

stress of wire-arc additive manufactured 2319 aluminum alloy [J]. Laser & Optoelectronics Progress, 2018, 55(1): 011413.

[144] GUO Wei, SUN Ru-jian, SONG Bin-wen, ZHU Ying, LI Fei, CHE Zi-gang, LI Bo, GUO Chao, LIU Lei, PENG Peng. Laser shock peening of laser additive manufactured Ti6Al4V titanium alloy [J]. Surface and Coatings Technology, 2018, 349: 503−510.

[145] LUO Si-hai, HE Wei-feng, CHEN Kai, Nie Xiang-fan, ZHOU Liu-cheng, LI Yi-ming. Regain the fatigue strength of laser additive manufactured Ti alloy via laser shock peening [J]. Journal of Alloys and Compounds, 2018, 750: 626−635.

[146] KALENTICS N, BOILLAT E, PEYRE P, ĆIRIĆ-KOSTIĆ S, BOGOJEVIĆ N, LOGÉ R E. Tailoring residual stress profile of selective laser melted parts by laser shock peening [J]. Additive Manufacturing, 2017, 16: 90−97.

[147] XING Xiao-dong, DUAN Xiao-ming, JIANG Ting-ting, WANG Jian-dong, JIANG Feng-chun. Ultrasonic peening treatment used to improve stress corrosion resistance of AlSi10Mg components fabricated using selective laser melting [J]. Metals, 2019, 9(1): 103.

[148] ZHOU Chang-ping, JIANG Feng-chun, XU De, GUO Chun-huan, ZHAO Cheng-zhi, WANG Zhen-qiang, WANG Jian-dong. A calculation model to predict the impact stress field and depth of plastic deformation zone of additive manufactured parts in the process of ultrasonic impact treatment [J]. Journal of Materials Processing Technology, 2020, 280: 116599.

[149] YANG Yi-chong, JIN Xin, LIU Chang-meng, XIAO Mu-zheng, LU Ji-ping, FAN Hong-li, MA Shu-yuan. Residual stress, mechanical properties, and grain morphology of Ti−6Al−4V alloy produced by ultrasonic impact treatment assisted wire and arc additive manufacturing [J]. Metals, 2018, 8(11): 934.

[150] ZHANG Mei-xia, LIU Chang-meng, SHI Xue-zhi, CHEN Xian-ping, CHEN Cheng, ZUO Jian-hua, LU Ji-ping, MA Shu-yuan. Residual stress, defects and grain morphology of Ti−6Al−4V alloy produced by ultrasonic impact treatment assisted selective laser melting [J]. Applied Sciences, 2016, 6(11): 304.

[151] BEZENÇON C, SCHNELL A, KURZ W. Epitaxial deposition of MCrAlY coatings on a Ni-base superalloy by laser cladding [J]. Scripta Materialia, 2003, 49(7): 705−709.

[152] KURZ W, BEZENÇON C, GÄUMANN M. Columnar to equiaxed transition in solidification processing [J]. Science and Technology of Advanced Materials, 2001, 2(1): 185−191.

[153] WANG Fu-de, WILLIAMS S, COLEGROVE P, ANTONYSAMY A A. Microstructure and mechanical properties of wire and arc additive manufactured Ti−6Al−4V [J]. Metallurgical and Materials Transactions A, 2013, 44(2): 968−977.

[154] WANG Ya-chao, SHI Jing. Microstructure and properties of Inconel 718 fabricated by directed energy deposition with in-situ ultrasonic impact peening [J]. Metallurgical and Materials Transactions B, 2019, 50(6): 2815−2827.

[155] DU Chang, ZHANG Jin, LIAN Yong, YUAN Xiao-min, MICHAEL Y H. Research status of residual stress in laser additive manufacturing [J]. Surface Technology, 2019, 48(1): 200−207.

[156] WALKER P, MALZ S, TRUDEL E, NOSIR S, ELSAYED M S A, KOK L. Effects of ultrasonic impact treatment on the stress-controlled fatigue performance of additively manufactured DMLS Ti−6Al−4V Alloy [J]. Applied Sciences, 2019, 9(22): 4787.

[157] GAO He, DUTTA R K, HUIZENGA R M, AMIRTHALINGAM M, HERMANS M J M, BUSLAPS T, RICHARDSON I M. Stress relaxation due to ultrasonic impact treatment on multi-pass welds [J]. Science and Technology of Welding and Joining, 2014, 19: 505−513.

[158] ZHOU Chang-ping, WANG Jian-dong, GUO Chun-huan, ZHAO Cheng-zhi, JIANG Guo-rui, DONG Tao, JIANG Feng-chun. Numerical study of the ultrasonic impact on additive manufactured parts [J]. International Journal of Mechanical Sciences, 2021, 197: 106334.

[159] HE Zhi, HU Yang, QU Hong-tao, WANG Zhi-min, BU Xian-zheng. Research on anisotropy of titanium alloy manufactured by ultrasonic impact treatment and wire and arc additive manufacture [J]. Aerospace Manufacturing Technology, 2016(6): 11−16. (in Chinese)

[160] CHEN Fu-rong, YANG Yi-hang, LI Nan. Effect of ultrasonic impact time on Microstructure and properties of 7A52 aluminum alloy tandem MIG welded joint [J]. The International Journal of Advanced Manufacturing Technology, 2021, 116(7): 2687−2696.

[161] ZHANG Qi, LI Mei-yan, HAN Bin, ZHANG Shi-yi, LI Yue, HU Chun-yang. Investigation on microstructures and properties of Al1.5CoCrFeMnNi high entropy alloy coating before and after ultrasonic impact treatment [J]. Journal of Alloys and Compounds, 2021, 884: 160989.

[162] LI Hao, WU Feng-he, ZHAO Feng, ZHANG Qing-long, LI Yi-fei. Effects of cavitation impact technology on cavitation erosion behavior of AA6061-T6 [J]. China Surface Engineering, 2021, 34(3): 83−89. (in Chinese)

[163] SONG Han-yu, LI Ming-lang, WANG Mu-xuan, WU Ben-xin, LIU Ze, DING Hong-tao, LIU Wei-dong. Preliminary experimental study of warm ultrasonic impact-assisted laser metal deposition [J]. Journal of Manufacturing Science and Engineering, 2021, 143(7): 074501.

[164] LESYK D A, MARTINEZ S, MORDYUK B N, DZHEMELINSKYI V V, LAMIKIZ A, PROKOPENKO G I. Post-processing of the Inconel 718 alloy parts fabricated by selective laser melting: Effects of mechanical surface treatments on surface topography, porosity, hardness and residual stress [J]. Surface and Coatings Technology, 2020, 381: 125136.

[165] ZHANG Shuai, ZHANG Ya-zhou, GAO Ming, WANG Fu-de, LI Quan, ZENG Xiao-yan. Effects of milling thickness on wire deposition accuracy of hybrid additive/subtractive manufacturing [J]. Science and Technology of Welding and Joining, 2019, 24(5): 375−381.

[166] LI Fang, CHEN Shu-jun, SHI Jun-bao, TIAN Hong-yu, ZHAO Yun. Evaluation and optimization of a hybrid manufacturing process combining wire arc additive manufacturing with milling for the fabrication of stiffened panels [J]. Applied Sciences, 2017, 7(12): 1233.

[167] MANOGHARAN G, WYSK R A, HARRYSSON O L A.

Additive manufacturing–integrated hybrid manufacturing and subtractive processes: economic model and analysis [J]. International Journal of Computer Integrated Manufacturing, 2016, 29(5): 473−488.

[168] DU Wei, BAI Qian, ZHANG Bi. A novel method for additive/subtractive hybrid manufacturing of metallic parts [J]. Procedia Manufacturing, 2016, 5: 1018−1030.

[169] DU Wei, BAI Qian, ZHANG Bi. Machining characteristics of 18Ni-300 steel in additive/subtractive hybrid manufacturing [J]. The International Journal of Advanced Manufacturing Technology, 2018, 95(5): 2509−2519.

[170] SONG Y A, PARK S, CHOI D, JEE H. 3D welding and milling: Part I—A direct approach for freeform fabrication of metallic prototypes [J]. International Journal of Machine Tools and Manufacture, 2005, 45(9): 1057−1062.

[171] SONG Y A, PARK S, CHAE S W. 3D welding and milling: Part II—Optimization of the 3D welding process using an experimental design approach [J]. International Journal of Machine Tools and Manufacture, 2005, 45(9): 1063−1069.

[172] SONG Y A, PARK S. Experimental investigations into rapid prototyping of composites by novel hybrid deposition process [J]. Journal of Materials Processing Technology, 2006, 171(1): 35−40.

[173] ZHANG Shuai, GONG Meng-cheng, ZENG Xiao-yuan, GAO Ming. Residual stress and tensile anisotropy of hybrid wire arc additive-milling subtractive manufacturing [J]. Journal of Materials Processing Technology, 2021, 293: 117077.

[174] SUNNY S, MATHEWS R, GLEASON G, MALIK A, HALLEY J. Effect of metal additive manufacturing residual stress on post-process machining-induced stress and distortion [J]. International Journal of Mechanical Sciences, 2021, 202/203: 106534.

[175] SALONITIS K, D'ALVISE L, SCHOINOCHORITIS B, CHANTZIS D. Additive manufacturing and post-processing simulation: laser cladding followed by high speed machining [J]. The International Journal of Advanced Manufacturing Technology, 2016, 85(9): 2401−2411.

# 金属材料电弧熔丝增材制造研究现状与质量改进方法

李彦朋[1,2]，王长瑞[1,3]，杜小东[4]，田 威[1]，张 涛[5,6]，胡俊山[1]，李 波[1]，李鹏程[1]，廖文和[7]

1. 南京航空航天大学 机电学院，南京 210016；
2. School of Aerospace, Transport and Manufacturing, Cranfield University, MK43 0AL, United Kingdom；
3. 哈尔滨工业大学 先进焊接与连接国家重点实验室，哈尔滨 150001；
4. 中国电子科技集团公司第二十九研究所，成都 610036；
5. 中南大学 轻合金研究院，长沙 410083；
6. 中南大学 高性能复杂制造国家重点实验室，长沙 410083；
7. 南京理工大学 机械工程学院，南京 210094

**摘 要**：电弧熔丝增材制造(WAAM)是一种增材制造技术，近年来在工业上有很大的发展潜力。总结目前 WAAM 的研究现状和面临的挑战，并提出质量改进的方法。综述 WAAM 在表面质量、成形精度、显微组织、力学性能、残余应力和变形、孔隙及其他缺陷等方面的研究现状。从前处理、在线处理和后处理 3 个方面总结消除缺陷、改善显微组织和提高力学性能的方法。WAAM 的广泛应用仍然存在许多挑战，可能需要从多个角度出发来实现 WAAM 的工业化应用。 路径规划和切片算法的开发、在线监测系统与现有 WAAM 设备的结合、后处理技术的复合等将是未来的重点研究方向。

**关键词**：电弧熔丝增材制造；材料性能改善；工艺参数控制；在线监测；后处理

**(Edited by Bing YANG)**